

INDUCED PLURIPOTENT STEM CELLS GENERATED FROM WISKOTT-ALDRICH SYNDROME
PATIENTS SHOWED DEFECTS IN PLATELET PRODUCTION IN VITRO

Miss Praewphan Ingrungruanglert



จุฬาลงกรณ์มหาวิทยาลัย
CHULALONGKORN UNIVERSITY

บทคัดย่อและแฟ้มข้อมูลฉบับเต็มของวิทยานิพนธ์ตั้งแต่ปีการศึกษา 2554 ที่ให้บริการในคลังปัญญาจุฬาฯ (CUIR)

เป็น Dissertation Submitted in Partial Fulfillment of the Requirements

for the Degree of Doctor of Philosophy Program in Medical Science

The abstract and full text of theses from the academic year 2011 in Chulalongkorn University Intellectual Repository (CUIR)

are the thesis authors' files submitted through the University Graduate School.
Faculty of Medicine

Chulalongkorn University

Academic Year 2014

Copyright of Chulalongkorn University

เซลล์ต้นกำเนิดที่สร้างได้จากการเหนี่ยวนำเซลล์ผิวหนังของผู้ป่วยโรค WISKOTT-ALDRICH SYNDROME แสดงความผิดปกติในกระบวนการสร้างเกล็ดเลือดในหลอดทดลอง

นางสาวแพรวพรรณ อิงรุ่งเรืองเลิศ



วิทยานิพนธ์นี้เป็นส่วนหนึ่งของการศึกษาตามหลักสูตรปริญญาวิทยาศาสตรดุษฎีบัณฑิต

สาขาวิชาวิทยาศาสตร์การแพทย์

คณะแพทยศาสตร์ จุฬาลงกรณ์มหาวิทยาลัย

ปีการศึกษา 2557

ลิขสิทธิ์ของจุฬาลงกรณ์มหาวิทยาลัย

Thesis Title INDUCED PLURIPOTENT STEM CELLS GENERATED
FROM WISKOTT-ALDRICH SYNDROME PATIENTS
SHOWED DEFECTS IN PLATELET PRODUCTION IN
VITRO

By Miss Praewphan Ingrungruangleert

Field of Study Medical Science

Thesis Advisor Assistant Professor Nipan Israsena, MD.Ph.D.

Accepted by the Faculty of Medicine, Chulalongkorn University in Partial
Fulfillment of the Requirements for the Doctoral Degree

.....Dean of the Faculty of Medicine
(Associate Professor Sophon Napathorn, MD.)

THESIS COMMITTEE

.....Chairman
(Professor Apiwat Mutirangura, MD.Ph.D.)

.....Thesis Advisor
(Assistant Professor Nipan Israsena, MD.Ph.D.)

.....Examiner
(Professor Kanya Suphapeetiporn, MD.Ph.D.)

.....Examiner
(Assistant Professor Amornpun Sereemaspun, MD.Ph.D.)

.....External Examiner
(Piya Rujkijyanont, MD.FAAP.)

แพรวพรรณ อิงรุ่งเรืองเลิศ : เซลล์ต้นกำเนิดที่สร้างได้จากการเหนี่ยวนำเซลล์ผิวหนังของผู้ป่วยโรค WISKOTT-ALDRICH SYNDROME แสดงความผิดปกติในกระบวนการสร้างเกล็ดเลือดในหลอดทดลอง (INDUCED PLURIPOTENT STEM CELLS GENERATED FROM WISKOTT-ALDRICH SYNDROME PATIENTS SHOWED DEFECTS IN PLATELET PRODUCTION IN VITRO) อ.ที่ปรึกษาวิทยานิพนธ์หลัก: ผศ. ดร. นพ. นิพัชญ์ อิศรเสนา ณ อยุธยา, 57 หน้า.

Wiskott Aldrich syndrome (WAS) เป็นโรคที่เกิดจากความผิดปกติทางพันธุกรรมของยีน WASP ที่อยู่บนโครโมโซม X WASP ทำหน้าที่ในการควบคุมกระบวนการสร้างสาย actin และ signal transduction แต่อย่างไรก็ดีหน้าที่ของ WASP ที่เกี่ยวข้องกับการเกิด microthrombocytopenia ซึ่งเป็นอาการเด่นของโรค WAS ยังไม่เป็นที่ทราบแน่ชัด การใช้หนูทดลอง และการใช้เซลล์ที่แยกได้จากผู้ป่วย WAS ไม่สามารถเลียนแบบความผิดปกติของเกล็ดเลือดของโรค WAS ได้ จึงไม่สามารถใช้โมเดลดังกล่าวในการศึกษาการเกิดโรคได้ ในการศึกษาครั้งนี้ทำการสร้าง WAS-iPSCs จากเซลล์ผิวหนังของผู้ป่วยโรค WAS จำนวน 2 คน โดยพบว่า hematopoietic progenitor cells ที่สร้างได้จาก WAS-iPSCs มีความสามารถในการเปลี่ยนแปลงไปเป็นเซลล์ในระบบเลือดไม่ต่างจาก iPSCs ที่สร้างได้จากคนปกติ ที่น่าสนใจคือ megakaryocytes ที่สร้างจาก WAS-iPSCs แสดงให้เห็นถึงความผิดปกติในการสร้าง proplatelet โดย proplatelet ที่สร้างได้จะมี proplatelet shaft ที่บาง มีการพองตัวของ platelet ในสายของ proplatelet ที่น้อยกว่าปกติ และจะพบ platelet buds ขนาดเล็กที่ปลายของ proplatelet ซึ่งจะสอดคล้องกับการสร้างเกล็ดเลือดขนาดเล็กที่พบใน WAS-iPSCs การแก้ไขความผิดปกติของยีน WASP ด้วยเทคนิค Zinc finger nuclease และการเพิ่มการแสดงออกของ WASP ให้กลับมามีการแสดงออกในระดับปกติสามารถแก้ไขความผิดปกติในการสร้าง proplatelet และแก้ไขความผิดปกติของขนาดเกล็ดเลือดได้ จากการทดลองนี้แสดงให้เห็นว่า WASP ทำหน้าที่เกี่ยวข้องกับการควบคุมการสร้าง proplatelet และขนาดของเกล็ดเลือด นอกจากนี้ยังได้ทำการทดสอบปลูกถ่ายเซลล์ Hematopoietic progenitor cells ที่สร้างจาก WAS-iPSCs ที่มีการแก้ไขความผิดปกติทางพันธุกรรม หลังจากการปลูกถ่ายสามารถตรวจพบเซลล์เม็ดเลือดขาวของมนุษย์ได้ในเลือดของหนูตัวรับ จากผลการทดลองทั้งหมดแสดงให้เห็นถึงความสามารถในการนำ iPSCs มาใช้เป็นโมเดลในการศึกษาโรคต่างๆในกระบวนการสร้างเกล็ดเลือด และยังใช้เป็นแหล่งของเซลล์ตั้งต้นสำหรับการปลูกถ่ายเพื่อการรักษาโรคในอนาคตได้อีกด้วย

สาขาวิชา วิทยาศาสตร์การแพทย์

ลายมือชื่อนิสิต

ปีการศึกษา 2557

ลายมือชื่อ อ.ที่ปรึกษาหลัก

5275365030 : MAJOR MEDICAL SCIENCE

KEYWORDS: WISKOTT-ALDRICH SYNDROME / INDUCED PLURIPOTENT STEM CELLS / WASP / THROMBOPOIESIS / PLATELET

PRAEWPHAN INGRUNGRUANGLERT: INDUCED PLURIPOTENT STEM CELLS GENERATED FROM WISKOTT-ALDRICH SYNDROME PATIENTS SHOWED DEFECTS IN PLATELET PRODUCTION IN VITRO. ADVISOR: ASST. PROF. NIPAN ISRASENA, MD.Ph.D., 57 pp.

Wiskott aldrich syndrome, an x-linked immunodeficiency disorder, caused by the mutation in WASP gene. WASP has been known as a regulator of actin reorganization in hematopoietic cells but its role in microthrombocytopenia, which is the hallmark of WAS, is largely unknown. Available WAS disease models failed to reproduced WAS platelet defects both in vivo and in vitro. In this study, we reported the generation of WAS-iPSCs from 2 patients with WASP mutation. Although, the hematopoietic and megakaryocytic differentiation potential of WAS-iPSC lines were comparable to the wild-type iPSCs, WAS-iPSC derived megakaryocytes exhibited abnormal proplatelet formation with thin proplatelet shaft, less in number of proplatelet branching and platelet swelling. Small size platelet buds at the proplatelet end observed in WAS-iPSCs correlated with their small platelet size. Restoration of WASP expression by lentiviral and isogenic model could rescued the defects in proplatelet formation and platelet size was increased. Our results showed for the first time that WASP play important roles in regulating proplatelet formation and controlling platelet size. Furthermore, xenotransplantation of hematopoietic progenitor cells derived from isogenic model showed multilineage engraftment including lymphoid lineage. Our result illustrated the potential of using iPSCs for modeling the disease mechanism in thrombopoiesis and serving as an unlimited cells source for future cell replacement therapy.

Field of Study: Medical Science

Student's Signature

Academic Year: 2014

Advisor's Signature

ACKNOWLEDGEMENTS

First and foremost, I would like to express my deepest gratitude to my advisor Asst. Prof. Nipan Israsena for the continuous support of my Ph.D. study and research, for his excellent guidance, patience, and motivation. Without him, my thesis would not have been completed. I would like to thank Prof. Vorasuk Shotelersuk and Prof. Kanya Suphapeetiporn for their support and encouragement. I also would like to thank my thesis committee Prof. Apiwat Mutirangura, Asst. Prof. Amornpun Sereemasapun and Dr. Piya Rujkijyanont for scarifying their time, insightful comments and suggestion.

My sincere thanks also go to Dr.Ruttachuk Rungsivivat for his help on iPSCs generation and iPSC culture.

My special thanks go to co-workers in Stem cells and cell therapy research unit for their helps and supports.

I would like to take this opportunity to thank Prof. Daniel Lacorazza and Chun Shik Park for the Xenotransplantation experiences, supporting and understanding during my stay in Houston.

The last, but not least, I deeply thank my family for their loves and supporting me throughout my life.

CONTENTS

	Page
THAI ABSTRACT	iv
ENGLISH ABSTRACT	v
ACKNOWLEDGEMENTS	vi
CONTENTS	vii
LIST OF FIGURE.....	ix
CHAPTER I INTRODUCTION.....	1
CHAPTER II BACKGROUND AND LITERATURE REVIEW.....	3
<i>Wiskott-aldrich syndrome (WAS)</i>	3
<i>Induced pluripotent stem cells: disease modeling and cell replacement therapy</i> .	7
<i>Platelet production and platelet size</i>	9
CHAPTER III MATERIALS AND METHODS	12
<i>Generation of iPSCs</i>	12
<i>Immunofluorescence staining</i>	13
<i>Reverse transcription-polymerase chain reaction (RT-PCR) and real-time PCR</i>	14
<i>Western blot for WASP expression</i>	15
<i>Colony forming cell (CFC) assay</i>	15
<i>Megakaryocyte differentiation</i>	16
<i>Flow cytometry analysis</i>	16

	Page
<i>Electron microscopic (EM) analysis of human iPSC-derived megakaryocytes and platelets</i>	17
<i>Xenotransplantation</i>	17
<i>Gene correction</i>	18
CHAPTER IV RESULTS	19
<i>Generation and characterization of WAS-iPSCs</i>	19
<i>Evaluation the effect of WASP mutation in early hematopoiesis</i>	20
<i>WAS-R iPSC derived megakaryocyte showed defect in maturation but not WAS-S</i>	24
<i>Isogenic model and WASP overexpression rescued small size platelets</i>	30
<i>Megakaryocytes derived from WAS-iPSCs exhibited defects in proplatelet formation.</i>	36
<i>WAS-iPSC derived megakaryocyte showed defect in actin reorganization</i>	39
<i>Xenotransplantation of iPSC derived CD34⁺ cells showed lymphoid engraftment</i>	41
CHAPTER V DISCUSSION	42
REFERENCES	48
VITA.....	57

LIST OF FIGURE

Figure 1 WASP structure and their auto inhibited form and active form.	5
Figure 2 Wiskott Aldrich syndrome functions in immune cell responses.....	6
Figure 3 The generation of patient specific pluripotent stem cells for disease modeling, drug screening and cell replacement therapy.....	8
Figure 4 Mechanism of proplatelet formation and platelet release.	10
Figure 5 Characterization of iPSCs.....	23
Figure 6 Epigenetic remodeling and pluripotency of iPSCs.....	23
Figure 7 Hematopoietic differentiation of WAS-iPSCs.	26
Figure 8 Hematopoietic progenitor cells generated from WAS-iPSCs showed defect in macrophage differentiation potential.....	27
Figure 9 WT-iPSCs and WAS-iPSCs generated similar numbers of megakaryocytes.....	28
Figure 10 Megakaryocytes generated from WAS-iPSCs..	29
Figure 11 Flow cytometry analysis of platelet-like particle produced in cultured supernatant.....	32
Figure 12 WAS-iPSCs produced small platelet size.....	33
Figure 13 Genetic correction of WASP gene in WASX503R-S by using ZFN technology.	34
Figure 14 Restored WASP expression rescued the defects observed in WAS-iPSC derived megakaryocytes.....	35
Figure 15 WAS-iPSC-derived megakaryocytes showed abnormal proplatelet structures.....	38
Figure 16 in vitro iPSCs differentiation for modeling large platelet disease.	39
Figure 17 Cytoskeleton reorganization in megakaryocytes derived from WAS-iPSCs...	40

Figure 18 Transplantation of iPSC derived CD34+ HPCs into humanized mice
showed T cell engraftment. 41



CHAPTER I

INTRODUCTION

Wiskott aldrich syndrome, rare X-linked recessive disease characterized by microthrombocytopenia, eczema, immunodeficiency, autoimmunity and increase the risk of malignancies(Orange, Stone et al. 2004), is caused by mutation in WAS protein (WASP). WASP specifically expresses in hematopoietic cells and has been known to play a role in actin reorganization and signaling transduction (Snapper and Rosen 1999; Thrasher and Burns 2010). WASP deficiency impaired immune cell responses which leading to recurrent of infection. Nonetheless, the underline molecular mechanism of WASP in microthrombocytopenia is still unknown.

In vitro culture of CD34⁺ cell isolated from WAS patients provided an inconclusive data. While some reported the defect in megakaryopoiesis and decreased in number of proplatelet forming cell (Kajiwara, Nonoyama et al. 1999), others showed that WAS derived megakaryocytes exhibited normal proplatelet formation with normal platelet size (Haddad, Cramer et al. 1999). In addition to human model, WASP deficient mice could not reproduced platelet defects, only mild thrombocytopenia were observed but the platelet size was normal (Sabri, Foudi et al. 2006). The megakaryocyte number in WASP deficient mice was increased with abnormal premature proplatelet formation in bone marrow.

The discovery of induced pluripotent stem cells in 2006 (Takahashi and Yamanaka 2006) provide an alternative unlimited cell source for disease modelling and cell replacement therapy as these cells are patient specific, easy to genetically modified and dividing indefinitely (Tiscornia, Vivas et al. 2011). Many disease specific iPSCs were generated from patients with genetic diseases and these cells exhibited

abnormal phenotypes in vitro (Lee, Papapetrou et al. 2009; Marchetto, Carromeu et al. 2010; Moretti, Bellin et al. 2010).

In this study, we reported the generation of WAS-iPSCs from two unrelated patients. WAS-iPSC derived megakaryocyte showed abnormal platelet formation with small platelet size. We demonstrated for the first time that the recovery of WASP expression using either ZFN mediated genetic correction or lentiviral containing WASP improved proplatelet formation and increased platelet size. Corrected WAS-iPSC derived hematopoietic progenitor cells showed multilineage engraftment including lymphoid lineage in recipient mice.



CHAPTER II

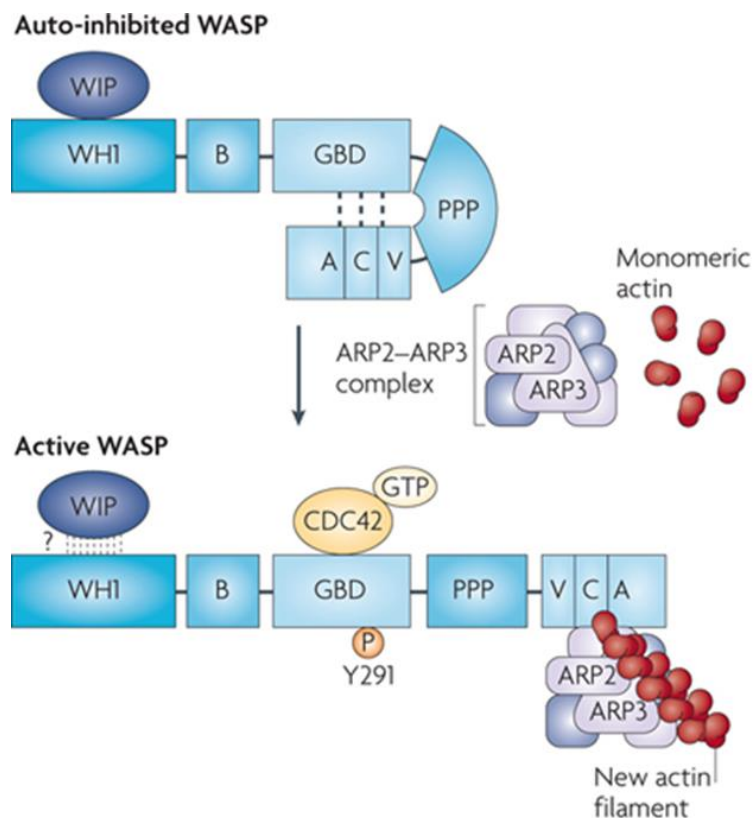
BACKGROUND AND LITERATURE REVIEW

Wiskott-aldrich syndrome (WAS)

Wiskott aldrich syndrome, rare X-linked recessive disease characterized by microthrombocytopenia, eczema, recurrent infection due to immunodeficiency, autoimmunity and increase the risk of malignancies (Bosticardo, Marangoni et al. 2009), was first described by Dr. Alfred Wiskott and Dr. Robert Anderson Aldrich (Wiskott et al. 1937)(Aldrich, Steinberg et al. 1954). WAS is caused by mutation in WAS protein (WASP) (Derry, Ochs et al. 1994). The missense mutations that inhibit less important function of WASP caused milder form, X-linked thrombocytopenia (XLT) that has only thrombocytopenia without infection (Zhu, Zhang et al. 1995; Albert, Bittner et al. 2010). Gain of function mutation in the region of WASP encoding the conserved GTPase binding domain (GBD) lead to X-linked severe congenital neutropenia (XLN) which has a different clinical features to WAS and XLT (Devriendt, Kim et al. 2001). WASP exclusively expresses in hematopoietic cells and has been known to play a role in actin reorganization and signaling transduction.

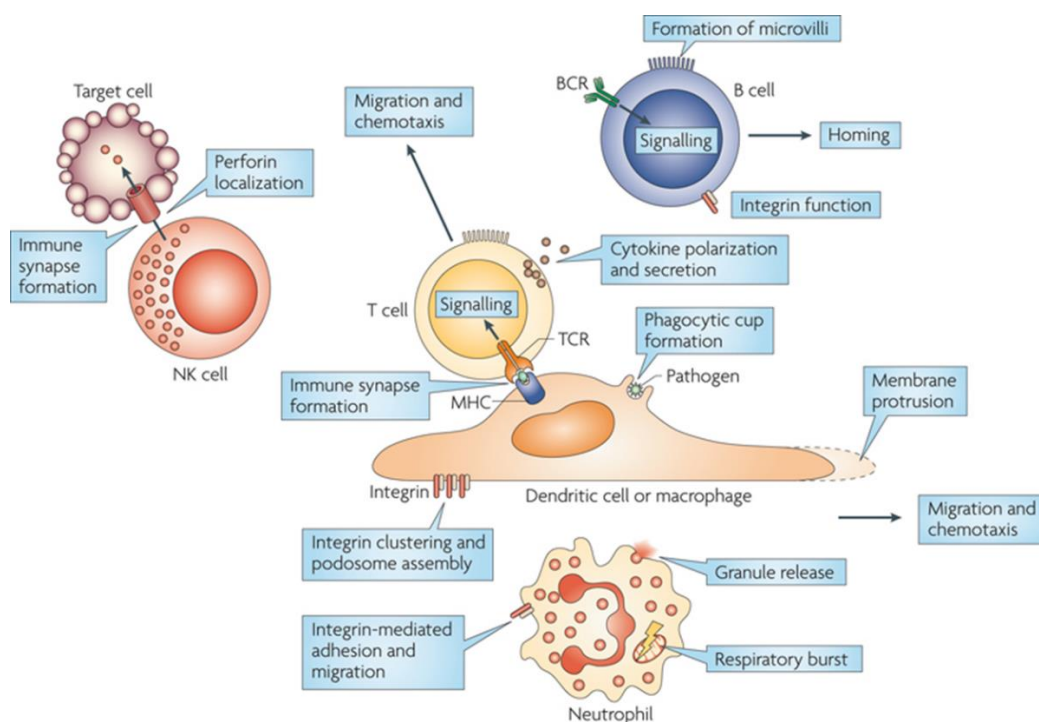
WAS gene located on the X chromosome, encoding WASP which contains 502 amino acid. WASP is the first identified member of a family of actin regulators including WASP, N-WASP (Miki, Miura et al. 1996), the WASP family verprolin homologous protein WAVE1, WAVE2 and WAVE3 (Bear, Rawls et al. 1998; Miki, Suetsugu et al. 1998; Suetsugu, Miki et al. 1999), WASP and SCAR homolog (WASH) (Linardopoulou, Parghi et al. 2007) and WASP homolog associated with membrane, actin and microtubule (WHAMM) (Campellone, Webb et al. 2008). These protein share common regions of homology called The VCA domain. WASP consists of multiple protein interacting domain, Ena-Vasp homology domain (EVH1 or WH1), a basic region (B), a Cdc42/Rac

GTPase binding domain (GBD), a proline rich domain, a G-actin binding verprolin homology domain (V), a cofilin homology domain (C) and the C-terminal acidic region (A). WASP functions as a platform for controlling actin polymerization. The auto inhibited form of WASP is mainly present in the cytoplasm in which the VCA domain interact with GBD, blocking the binding site for Arp2/3 actin-nucleating complex (Kim, Kakalis et al. 2000). Binding of the Rho-family GTPase, Cdc42, to GBD induce the conformational change and release the VCA domain, enable the binding of Arp2/3 complex to CA domain and mediated actin filament branching. The phosphorylation of tyrosine residue 291 in GBD stabilizes the open molecular conformation of WASP and enables maximum actin polymerization in the Cdc42 dependent manner (Torres and Rosen 2006). Actin cytoskeleton play an important role in many cellular function that involved in the immune response. Thus, in the absence of WASP immune cell functions including cell migration due to the chemotaxis, immune synapse formation and cell proliferation which required function and dynamic cytoskeleton rearrangement, are compromised (Molina, Sancho et al. 1993; Zhang, Shehabeldin et al. 1999; Dupre, Aiuti et al. 2002; Okabe, Fukuda et al. 2002; Orange, Ramesh et al. 2002). In contrast to immune cell defects, the underline molecular mechanism of WASP in microthrombocytopenia, the major cause of death in WAS (Sullivan, Mullen et al. 1994), is still unknown.



Nature Reviews | Immunology

Figure 1 WASP structure and their auto inhibited form and active form. WASP consists of 5 domains, WH1, B, GBD, proline rich and VCCA domain. In auto inhibited form binding of VCA to GBD restricts the binding of Apr2/3 complex. After interaction of Cdc42 to GBD which releases the VCA domain allow the binding of actin polymerizing machinery (Thrasher and Burns 2010)



Nature Reviews | Immunology

Figure 2 Wiskott Aldrich syndrome functions in immune cell responses (Thrasher and Burns 2010)

Transplantation of HLA-matched hematopoietic stem cells is the only curative therapy for WAS. In WAS patients with unrelated matched donor, HSC gene therapy provides as an alternative therapeutic strategy (Hacein-Bey-Abina, Le Deist et al. 2002). Gene therapy using retroviral (Boztug, Schmidt et al. 2010; Braun, Boztug et al. 2014) and lentiviral (Boztug, Schmidt et al. 2010; Hacein-Bey Abina, Gaspar et al. 2015) showed stable engraftment with improved in immune responses and platelet counts. Unfortunately, 7 of 10 WAS patients with retroviral gene therapy developed acute leukemia 4-10 years after transplantation.

Induced pluripotent stem cells: disease modeling and cell replacement therapy

Mouse models have been the gold standard for studying the mechanism underlying human genetic diseases by the advantage that mice share almost the same set of gene with human and can be genetically modified. However, many mouse models do not reproduce the phenotype observed in human due to the different between mouse and human biology (Sabri, Foudi et al. 2006; Odom, Dowell et al. 2007). The rarity of human stem cells and the difficulty to obtain human tissues limit the potential of using these cells for modeling human diseases. The discovery of induced pluripotent stem cells whereby somatic cells could reprogrammed back to the pluripotent state by introducing of specific transcription factors (Takahashi, Tanabe et al. 2007), provide an alternative unlimited cell source for disease modelling and cell replacement therapy as these cells are patient specific, easy to genetically modified and dividing indefinitely. iPSCs have potential to differentiate into all cell types in human body. A number of iPSCs are being generated from somatic cells of many patients. However, the epigenetic memory (Kim, Doi et al. 2010), interline variability (Soldner and Jaenisch 2012), reprogramming efficiency and differentiation protocol have been proposed as obstacles in using iPSCs for disease modeling (Inoue, Nagata et al. 2014).

The efficient differentiation method also critical in generation of sufficient amount of disease relevant cell type from iPSCs for modeling disease (Tiscornia, Vivas et al. 2011). For studying platelet diseases, there are two groups reported the efficient protocol on generating functional platelets from human pluripotent stem cells (hPSCs) (Takayama, Nishikii et al. 2008; Lu, Li et al. 2011). Platelets derived from hPSCs had ability to form blood clotting both in vitro and in vivo. Thus, these provide the opportunity to studies platelet biogenesis and the defects by using iPSCs.

In order to eliminate the confounding of genetics background, generation of isogenic line in which their genetics are identically matched to the parental line except

the disease causing mutation, by using nuclease technology such as, Zinc finger nuclease (ZFN) (Maeder, Thibodeau-Beganny et al. 2008) , transcription activator like effector nucleases (TALENs) (Miller, Tan et al. 2011) and clustered regulatory interspaced short palindromic repeat (CRISPR)/Casbased RNA-guided DNA endonucleases (Mali, Yang et al. 2013) is gaining momentum (Kim, Bernitz et al. 2014). Furthermore, mutation corrected isogenic iPSCs potentially to be used as a cell source for future cell replacement therapy.

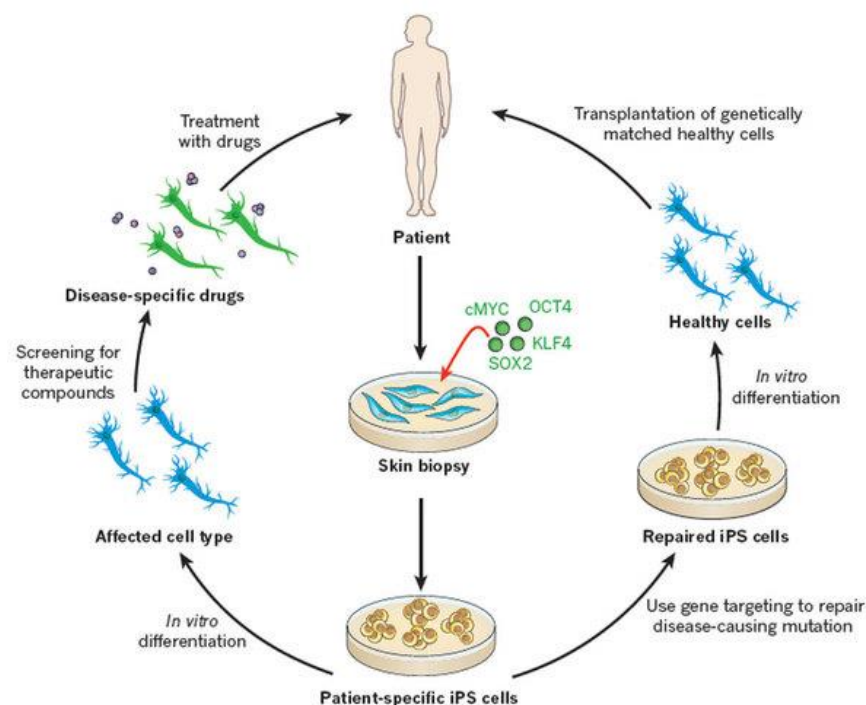


Figure 3 The generation of patient specific pluripotent stem cells for disease modeling, drug screening and cell replacement therapy (Robinton and Daley 2012).

iPSC based technology provides an unlimited cell source for clinical translation. Nonetheless, for example, developmental state of hematopoietic cells divide into two parts, primitive and definitive hematopoiesis. Mostly hematopoietic progenitor cells differentiated from pluripotent stem cells showed the primitive phenotypes in which nucleated and enucleated erythrocytes were generated with the expression of fetal hemoglobin but not adult (Miharada, Hiroyama et al. 2006; Hiroyama, Miharada et al.

2008). Moreover these cells exhibited the inability to engraft and reconstituted human cells in bone marrow of humanized mice that delayed the use of PSC derived blood cells for future replacement therapy (Ledran, Krassowska et al. 2008; Risueno, Sachlos et al. 2012; Doulatov, Vo et al. 2013).

Platelet production and platelet size

Platelets are small (2-4 microns in diameter), anucleated discoid cell fragments that responsible for hemostasis maintenance. Platelet size and number are critical parameters for their function in vivo. Abnormal bleeding is a major cause of death in patient who has macro- or microthrombocytopenia. We are now known that, platelets are generated from megakaryocytes, which reside in the bone marrow. However the mechanisms that control platelet size and platelet production are remain unclear.

The proplatelet model, megakaryocytes release platelets into bloodstream by extend long processes of its cytoplasm called “proplatelet”, toward sinusoidal blood vessel of bone marrow. Spontaneous megakaryocytes elaborated proplatelet formation also detects in culture of human and mouse derived cells. Proplatelet fragmentation, both in vivo and in vitro, releases heterogeneous mix population that larger than platelet size (2-10 micron in diameter) name as “preplatelet”. Preplatelet can reversibly convert into barbell shape proplatelet which then undergo abscission and yield two individual mature platelets (Patel, Hartwig et al. 2005; Hiroyama, Miharada et al. 2008; Thon, Montalvo et al. 2010).

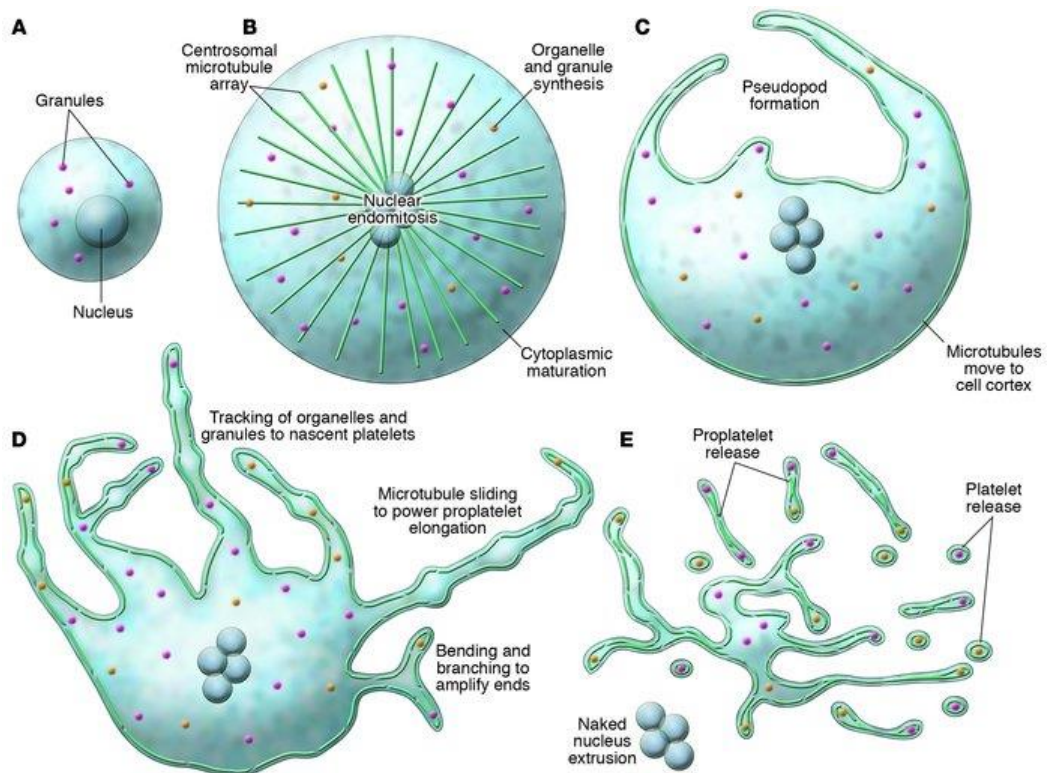


Figure 4 Mechanism of proplatelet formation and platelet release. (A) Megakaryocyte (B) undergo endomitosis and synthesis of organelles and granules. (C) The formation of pseudopod and (D) extension of proplatelet processes (E) platelet release (Patel, Hartwig et al. 2005).

Cytoskeletons are known to play important roles in thrombopoiesis and platelet release. Microtubule elongation and sliding driven the extension of proplatelet, pre-proplatelet conversion, formation of platelet bud at proplatelet tip and transportation of granules, organelles to the buds (Italiano, Lecine et al. 1999; Schwer, Lecine et al. 2001). Microtubule coil diameter and thickness at proplatelet end are associated with terminal platelet size and its discoid shape (Thon, Macleod et al. 2012). Inhibition of microtubule assembly in megakaryocytes block the formation of proplatelets (Tablin, Castro et al. 1990; Italiano, Lecine et al. 1999). In $\beta 1$ -tubulin knockout mice, platelets are spherical and the number of microtubule coil are reduced. These mice have thrombocytopenia with platelet count lower than 50% of normal mice. Large spherical platelet with abnormal microtubule coil also observe in

human patient who has a mutation in β 1-tubulin gene (Tablin, Castro et al. 1990; Freson, De Vos et al. 2005).

Actin is the most abundant cytoskeleton proteins which play an important role in many cellular processes. However, the role of actin in proplatelet formation and platelet release are largely unknown. Bending and branching of proplatelet in order to amplification of platelet free end has been reported to depend on actin polymerization. Megakaryocytes treated with cytochalasin B, and D, potent actin polymerization inhibitors, showed abnormal in proplatelet branching (Italiano, Lecine et al. 1999).



CHAPTER III

MATERIALS AND METHODS

Generation of iPSCs

Dermal fibroblasts from two previously reported WAS patients (Chatchatee, Srichomthong et al. 2003; Amarinthnukrowh, Ittiporn et al. 2013) and two unrelated normal individuals were obtained from skin biopsies. Studies using human cells were approved by the institutional review board of the Faculty of Medicine of Chulalongkorn University and were conducted in accordance with the Declaration of Helsinki.

ReV-iPSCs were generated using the following methods. 6×10^6 GP-293 cells were transfected with 13 μg of each retroviral vector (Addgene, Cambridge, MA), pMIG-OCT4 (clone 17225), pMIG-SOX2 (clone 17226), pMIG-KLF4 (clone 17227), pMXS-cMYC (clone 13375), and 5 μg of pVSV-G (Clontech, Palo Alto, CA) using X-tremeGENE HP DNA Transfection Reagent (Roche, Indianapolis, IN). 48 hours after transfection, the media were collected and filtered through a 0.45- μm pore size filter. Virus-containing supernatants were centrifuged at 25,000 rpm for 90 minutes. Viral pellets were resuspended with Opti-MEM (Invitrogen, Carlsbad, CA). Human fibroblasts were transduced with the OKSM retrovirus cocktail supplemented with 6 $\mu\text{g}/\text{mL}$ polybrene. Five days after transduction, transduced fibroblasts were seeded onto mitotically inactivated human foreskin fibroblasts and cultured with iPS media until an emerging of iPS colonies.

SeV-iPSCs were generated by using temperature sensitive Sendai virus (SeV) vectors (TS7) encoding Oct-3/4, Sox2, Klf4 and c-Myc (a gift from DNAVEC, Japan). The reprogramming procedure was performed as previously described (Fusaki, Ban et al. 2009; Ban, Nishishita et al. 2011; Nishishita, Shikamura et al. 2012).

Chula2, a human embryonic stem cell (hESC) line (Pruksananonda, Rungsiwiwut et al. 2012), was used as a control.

To generate lentiviral vectors expressing WASP, the WASP coding sequence was cloned into the pLenti6.3/TO/V5-DEST (Invitrogen) using LR Clonase® II (Invitrogen). 293FT cells were transfected with 5 μg of each pLenti6.3/TO/WASP, pLP1, pLP2 and pVSV-G (Invitrogen) using X-tremeGENE HP DNA Transfection Reagent (Roche). Two days after transfection, the media were collected and filtered through a 0.45- μm pore size filter. Virus-containing supernatants were centrifuged at 25,000 rpm for 90 minutes. Viral pellets were resuspended with Opti-MEM (Invitrogen). Hematopoietic progenitor cells from ES-sacs on day 14 were transduced with lentiviruses supplemented with 6 $\mu\text{g}/\text{mL}$ polybrene. 24 hours after transduction, cells were reseeded onto mitotically inactivated OP9 feeder cells and cultured in the megakaryocyte differentiation medium.

Immunofluorescence staining

Human iPSCs were fixed with 4% formaldehyde for 15 minutes at room temperature and then permeabilized with 1XPBS supplemented with 0.3% Triton X-100 for 15 minutes. Human iPSCs were then blocked in blocking solution (10% goat serum and 0.3% Triton X-100 in PBS) for 30 minutes at room temperature and stained with primary antibodies, Oct4, Nanog, Tra-1-60, Tra-1-181 (StemLiteTMPluripotency IF kit, Cell Signaling, Danvers, MA) at 4oC overnight. Cells were stained with the Alexa Fluor conjugated secondary antibody (Molecular Probes, Invitrogen) for 1 hour. For Sendai virus detection, anti-Sendai virus (PD029, Medical & Biological Laboratories Co., Ltd., Japan) was used as a primary antibody.

For platelet staining, platelet-containing supernatant containing 1 μM prostaglandin E1 was centrifuged at 2000 rpm. Platelet pellet was resuspended and smeared onto the poly-L-lysine coated cover slide and dried. For proplatelet staining,

iPSC-derived megakaryocytes on day 21 of culture were reseeded onto coverslips coated with matrigel and cultured for 24 hours. Then, slides were fixed with 4% formaldehyde for 15 minutes at room temperature and then permeabilized with 1XPBS supplemented with 0.3% Triton X-100 for 15 minutes. Proplatelets and platelets were then blocked in the blocking solution for 30 minutes at room temperature and stained with anti- α -tubulin (Abcam, Cambridge, MA) and phalloidin-FITC (Molecular Probes, Invitrogen). For WASP overexpression experiment, proplatelets were stained with anti-WASP (Abcam) and phalloidin-FITC, and platelets were stained with anti-WASP (Abcam) and anti- α -tubulin (Abcam). For F-actin staining, iPSC-derived megakaryocytes on day 24 of culture were re-plated onto coverslips coated with collagen type I and cultured for 2 hours. Then, cells were fixed, permeabilized and blocked. Cells were subsequently stained with anti CD42b-PE (BioLegend, San Diego, CA) and phalloidin-FITC. 1 μ g/mL DAPI (Molecular Probes, Invitrogen) was used for nuclear staining. All fluorescence images were obtained by using Axio Observer fluorescence microscope (Carl Zeiss, Germany). The shortest diameter of tubulin-stained discoid-shaped platelets was measured by using AxioVision Rel 4.8 (Carl Zeiss).

Reverse transcription-polymerase chain reaction (RT-PCR) and real-time PCR

Total RNA was extracted by using TRI reagent (Molecular Research Center, Cincinnati, OH). Isolated RNA was reverse transcribed with RevertAid™ H Minus M-MuLV (Fermentas, Glen Burnie, MD). Real-time PCR assay was performed by using Maxima SYBR Green/ROX qPCR Master Mix (2X) (Fermentas) on ABI 7500 Fast Real-Time PCR System.

Western blot for WASP expression

40 micrograms of total protein lysates were mixed with 6X loading dye, Laemmli sample buffer, boiled at 95°C for 5 minutes, and loaded onto 10% sodium dodecylsulfate polyacrylamide gel. A mouse anti-WASP monoclonal antibody raised against a recombinant protein corresponding to the N-terminal region of human WASP (B-9; Santa Cruz Biotechnology, Santa Cruz, CA) and a goat anti-mouse IgG2a-HRP (sc-2005; Santa Cruz Biotechnology) were used as primary and secondary antibodies, respectively. GAPDH was used as a control for protein loading.

Colony forming cell (CFC) assay

All hematopoietic progenitor assays were performed according to the manufacturer's instructions (STEMCELL Technologies, Vancouver, Canada). Briefly, 16,500 progenitor cells were added to 3.3 mL of methylcellulose media (MethoCult™ H4034 Optimum) and mixed. Then, 1 mL of methylcellulose media containing cells was plated onto a 35-mm petri dish in duplicate using a 3-mL syringe attached to a 16 gauge blunt-end needle. Methylcellulose cultures were incubated for 12 to 14 days at 37°C in a humidified incubator with 5% CO₂. The total number of colonies per dish was scored on day 12 to 14. Human megakaryocyte progenitors were analyzed using MegaCult®-C (STEMCELL Technologies). 4,400 progenitor cells were added to 2 mL MegaCult®-C media with cytokines. 1.2 mL of cold collagen solution was then added. 0.75 mL of the final culture mixture was dispensed into each of the two wells of a double chamber slide. On day 12, cultures were dehydrated, fixed and stained for the detection of megakaryocyte progenitors.

Megakaryocyte differentiation

Human iPSCs were dissociated into small pieces (>100 cells) by collagenase treatment. Small clumps of human iPSCs were transferred onto mitotically inactivated OP9 cells and cultured in a hematopoietic cell differentiation medium, IMDM supplemented with a cocktail of 10 $\mu\text{g}/\text{mL}$ human insulin, 5.5 $\mu\text{g}/\text{mL}$ human transferrin, 5 ng/mL sodium selenite, 2 mM L-glutamine, 0.45 mM α -monothioglycerol, 50 $\mu\text{g}/\text{mL}$ ascorbic acid, 15% FBS and 20 ng/mL human vascular endothelial growth factor (VEGF; R&D system, Minneapolis, MN) (Figure 1A). 14 days after differentiation, cells were collected and gently crushed with a pipette and passed through a 40- μm cell strainer to obtain hematopoietic progenitors, which were transferred onto freshly irradiated feeder cells and cultured in the hematopoietic cell differentiation medium supplemented with 50 ng/mL human thrombopoietin (TPO; R&D system), 10 ng/mL human stem cell factor (SCF; R&D system) and 25 ng/mL heparin (Sigma-Aldrich, St Louis, MO). The non-adherent cells were collected and analyzed on day 24.

Flow cytometry analysis

Progenitor cells isolated from ES-sacs were stained with APC-conjugated anti-human CD34 (BD Biosciences, San Jose, CA) and PerCP-conjugated anti-human CD45 (BD Biosciences) for hematopoietic cell analysis on day 14 of differentiation. FITC-conjugated anti-human CD41a (BioLegend) and PE-conjugated anti-human CD42b (BioLegend) were used to detect megakaryocyte differentiation and platelet-like particles. Stained cells were analyzed by using BD FACSAria II (Becton Dickinson, Franklin Lakes, NJ). For platelet analysis, platelet-like particles in culture supernatant were gated by using same FSC and SSC as normal platelet. The number of CD41a+ CD42b+ megakaryocytes and platelet-like particles was counted by using CountBright™ Absolute Counting Beads (Molecular Probes, Invitrogen).

Electron microscopic (EM) analysis of human iPSC-derived megakaryocytes and platelets

Human iPSC-derived megakaryocytes and platelets were gently collected on day 24 as previously described (20). Briefly, one-ninth volume of acid citrate dextrose solution was added and centrifuged at 150g for 10 minutes to collect megakaryocytes. The supernatant was transferred to a new tube. 1 μM prostaglandin E1 and 1 U/mL apyrase were added. The supernatant containing platelets was centrifuged at 400g for 10 minutes to sediment the platelets. Megakaryocytes and platelets were then fixed with 3% glutaraldehyde at 4°C for 60 minutes and post-fixed with 2% osmium tetroxide in phosphate buffer at 4°C for 60 minutes. Specimens were then dehydrated in ethanol and embedded in 100% resin at 60°C for 48 hours. Thin sections were cut on an ultramicrotome and collected on mesh copper grids, stained with uranyl acetate and lead citrate. All images were examined by electron microscopy (JEOL 1210, JEOL, Tokyo, Japan). The shortest diameter of platelet particles containing alpha granules (A), dense core granules (D) and open canalicular systems (OCS) on whole mesh copper grid was measured by Image Pro Plus (Nikon, Tokyo, Japan).

Xenotransplantation

NSG mice were purchased from The Jackson Laboratory. Mice were sublethally irradiated at 365 rad using X-ray 4 hour before injection. Mice were anesthetized in induction chamber by using anesthetic vaporizer (Vaporizer generated mixer of Oxygen:Isoflurane, Oxygen flow 0.5 l/min and 3% isoflurane). Mouse were taken out from the induction chamber and placed on nose cone for maintaining anesthesia. Mouse skin was wiped by using 70% EtOH. Fur at the knee joint area was removed. Knee was flexed to 90 degree. 27-G needle was placed at the end of femur and twisted gently to make a tunnel into bone marrow cavity. 28-G needle syringe filled with 10^5 HPCs was then inserted into the bone marrow cavity and cells were injected. Mouse

was removed from nose cone and injected with Buprenorphine (1mg/kg). Mouse was placed in a warmed cage for recovery after procedure. Blood analysis were performed every two months by retro-orbital bleeding.

Gene correction

WAS-iPSCs were dissociated into single cells using accutase. 5 million iPSC cells were then resuspended into 100 ul P3 nucleofection solution. 5ug of Donor vector and + 5 ug of each ZFN vectors were added to cell suspension. Cell solution was then transferred to cuvette and nucleofected using preset program for human embryonic stem cells on the Amaxa Nucleofector IV. Transfected iPSCs were culture on mitotically inactivate DR4 feeder cells in mTeSR1 media supplemented with 10uM Y-27632. Media was changed every day. 10 ug/ml hygromycin was added to culture media at day 3 after transfection. Hygromycin concentration was increased to 20 ug/ml at day 5. At day 10-14, Hygromycin resistance colonies were picked and expanded. WASP correction was confirmed by DNA sequencing. For cre recombination, corrected WAS-iPSCs were seeded and transfected with cre recombinase mRNA. The excision of selection cassette was tested by treated with hygromycin. Non-resistance iPSCs were selected as Cre-corrected WAS-iPSCs.

CHAPTER IV

RESULTS

Microthrombocytopenia is the hallmark of Wiskott Aldrich syndrome, however, available disease models fail to reproduce the small size platelets both in vivo and in vitro. The discovery of iPSCs provide the opportunity to be used as disease modeling. Although, these cells can be patient specific and have ability to differentiate into all cell types including hematopoietic cell lineage, there is no evidence whether iPSCs could recapitulate platelet defects in vitro.

Generation and characterization of WAS-iPSCs

To validate whether iPSCs generated from WAS patient's fibroblasts are pluripotent, iPSCs were derived from fibroblasts of two WAS patients and two healthy controls. In this study, two reprogramming method both integrating and non-integrating were used. Four iPSC lines, WT-R#1, WT-R#2, WASX503-R#1 and WASX503R#2 were generated by using retrovirus encoding OCT4, SOX2, Klf4 and c-MYC. Other 7 iPSC lines, WT-S, WASX503R-S#1, WASX503R-S#2, WASQ19X-S#1, WASQ19X-S#2, WASQ19X-S#3, WASQ19X-S#4 were generated by using Temperature sensitive strain (TS7) Sendai virus. To test whether all selected iPSCs were completely reprogrammed, the absence of exogenous genes expression in retroviral group was confirmed by RT-PCR (Figure 5B) and the lack of residual SeV after treatment at 38°C were checked by immunofluorescence staining (Figure 5C). To examine epigenetic reprogramming of pluripotent gene promoter, OCT4 and NANOG , bisulfite sequencing were performed. We found that methylation of OCT4 and NANOG promoter were absented in WT-iPSCs and WAS-iPSCs similar to hES control (Figure 6A). The expression of pluripotent genes were analyzed by RT-PCR and immunofluorescence (Figure 5B, D and E). All 11 iPSC lines expressed pluripotent genes, OCT4, Nanog, TRA-1-60 and TRA-1-81. The

pluripotency of iPSCs were tested by teratoma formation. All iPSCs had the ability to differentiate into cells within three germ layer, ectoderm, mesoderm and endoderm (Figure 6B). All these data indicated that iPSC lines used in this study were pluripotent.

Evaluation the effect of WASP mutation in early hematopoiesis

The iPSC based modeling allowed us to study various state of hematopoiesis, as these cells could differentiate along the developmental line. WASP has been exclusively detected in the cells of hematopoietic lineage, including CD34⁺ progenitor cells. To study the role of WASP during early hematopoietic differentiation, iPSCs were differentiated into blood cell lineage using ES-SAC method (Figure 7A). Using western blot analysis, the expression of WASP was observed in WT-iPSC derived hematopoietic cells but not in WT-fibroblasts and WT-iPSCs. WASP was not detected in WAS-iPSCs derived hematopoietic cells (Figure 7B). After coculture with OP9 feeder cells, in the present of vascular growth factor (VEGF), both WT and WAS-iPSC iPSC formed SAC structures (Figure 7C). The number of CD34⁺ CD45⁻ progenitor cells produced within SACs were analyzed by flow cytometry (Figure 7D). There was no significant different in the percentage of CD34⁺ CD45⁻ of WT and WAS groups. To assess whether these cells have the ability to differentiate into myeloid lineages, colony forming assay was performed. No significantly different in number of cell capable to produce hematopoietic colonies between WT-iPSCs and WAS-iPSCs were observed (Figure 7E). WAS-iPSC derived hematopoietic progenitor cells can generated all colony types including BFU-E, CFU-E, CFU-G, CFU-M, CFU-GM and CFU-GEMM. These result indicated that in the absence of WAS, there was no defect in early hematopoietic differentiation which similar to what observed in the previous studies using CD34⁺ cord blood and bone marrow cells from WAS patients. Notably, consistent reduction of CFU-M colony number in WAS group were detected. This data suggested the potential defect in granulocyte/monocyte lineage decision. To assess macrophage differentiation

potential, hematopoietic progenitor cells were cultured in methycellulose media supplemented with M-CSF. Interestingly, the reduction of macrophage number and colony size was observed in WAS-iPSC derived hematopoietic progenitor cells (Figure 8). This finding might describe neutropenia observed in patient who has constitutively WASP activation. Further studies are required to address this issue.



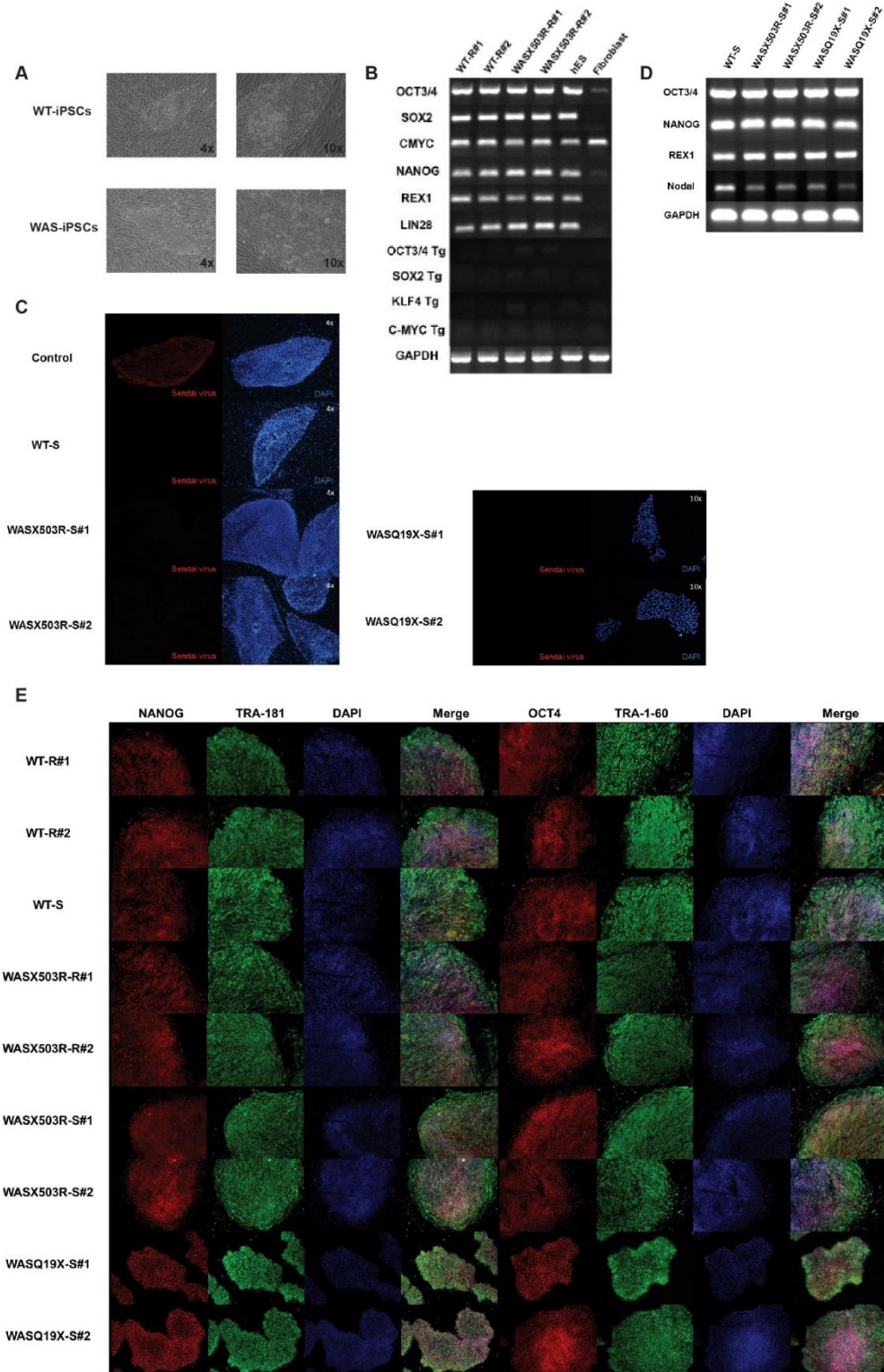


Figure 5 Characterization of iPSCs. (A) WT-iPSCs and WAS-iPSCs colony morphology observed under phase contrast microscope. RT-PCR analysis demonstrating that (B) hES (Chula2), WT-R iPSCs, WASX503R-R iPSCs (D) all SeV-iPSCs express pluripotency markers. Exogenous expression of Oct4, SOX2, Klf4 and c-Myc were undetectable. (C) Immunofluorescence staining of untreated SeV-iPSCs. All established SeV-iPSC lines were negative for sendai virus. (E) Immunofluorescence staining showing expression of pluripotency markers (TRA-1-60, TRA-1-81, Oct4 and Nanog) in WT-iPSCs and WAS-iPSCs. DAPI (blue) was used for nuclear staining. All iPSC lines are pluripotent.

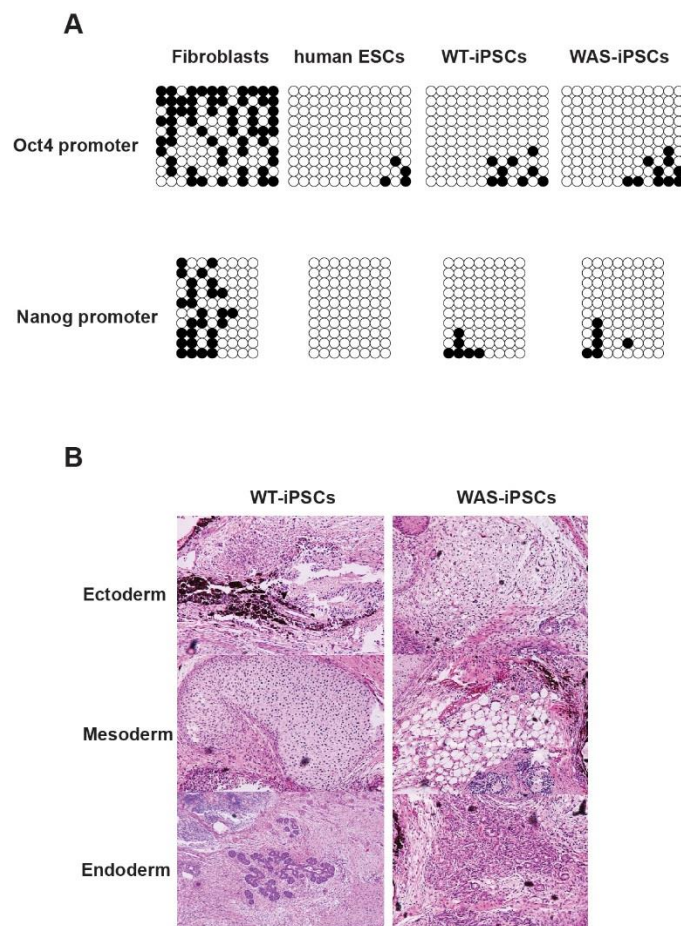


Figure 6 Epigenetic remodeling and pluripotency of iPSCs (A) Methylation at Oct4 and Nanog promoter were analyzed using bisulfite sequencing. (B) Teratoma formation of WT-iPSCs and WAS-iPSCs.

WAS-R iPSC derived megakaryocyte showed defected in maturation but not WAS-S

There was controversial on megakaryopoiesis in WAS. Some report demonstrated the decrease in megakaryocyte differentiation and maturation while most of study have not found such defects. To assess megakaryocyte differentiation potential, 1000 ES-sac derived progenitor cells were cultured in collagen-based megakaryocyte culture media. After 10 day Ten day after culture, CD41 positive colonies were counted. The number of CFU-MK in WT and WAS groups were not significantly different (Figure 9A). These data indicated that WASP did not play an important role in the differentiation step of HPC to megakaryocyte progenitor. Next, the process of megakaryocyte maturation was examined. Cells from ES-sac were additionally cultured on OP9 feeder cell in the presented of SCF and TPO for 10 days (day24). The number of CD41⁺ CD42b⁺ cells were analyzed at day 18, 21 and 24 of differentiation. Remarkably, the higher percentage of CD41⁺ CD42b⁺ megakaryocytes at day 21 and 24 were detected in WASX503R-R#1 and 2 (Figure 9B and C). These cells seem to stay in proliferation state longer than the rest. As previous reports, size and ploidy of iPSCs derived megakaryocytes in our study was less than those generated from cord blood and bone marrow cells. During megakaryocyte maturation, megakaryocyte specific granules were synthesized and demarcation membrane system was developed. The ultrastructure of megakaryocytes were analyzed using electron microscope (EM). The results showed that megakaryocytes derived from WT-R#1, WT-S, WASX503R-S#1, WASQ19X-S#1 but not WASX503R-R#1 exhibited well-developed demarcation membrane system throughout their cytoplasm (Figure 10). Poorly-developed demarcation membrane system was observed in very few WASX503R-R#1 derived megakaryocytes. In addition, the number of granules in megakaryocytes derived from WASX503R-R#1 was significantly lower compared to other iPSC groups. The abnormalities detected in WASX503R-R#1 derived megakaryocytes were similar to previous studies using megakaryocytes generated from peripheral blood and bone marrow of WAS patients.

Interestingly, the abnormalities described above were not observed in megakaryocytes derived from WAS-iPSCs generated with sendai virus, the defects in WASX503R-R probably caused by the reprogramming method.



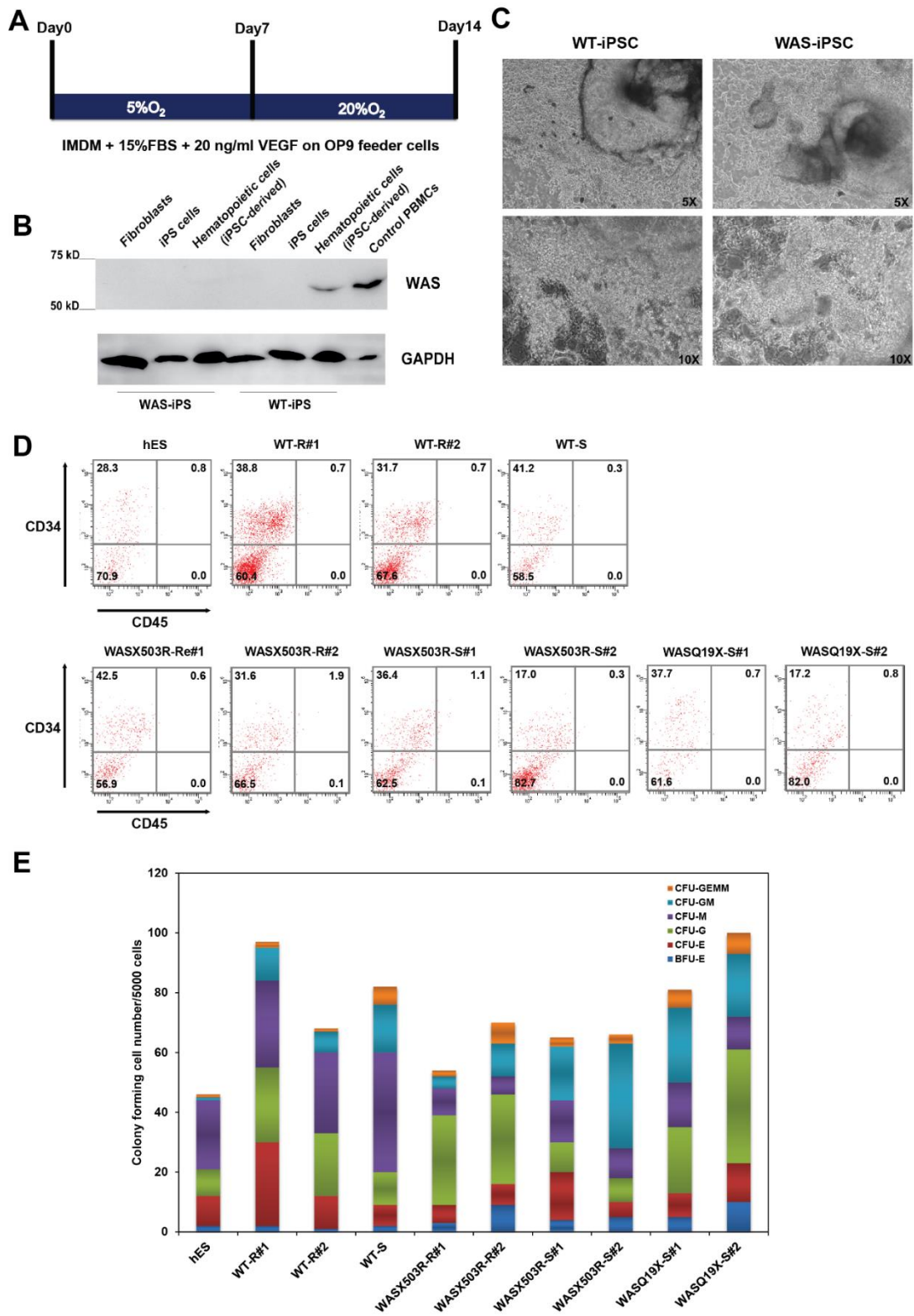


Figure 7 Hematopoietic differentiation of WAS-iPSCs. (A) Schematic diagram of *in vitro* differentiation protocol. (B) Western blot analysis showing WASP expression in

hematopoietic cells derived from WT-iPSCs (WT-R#1) but not in fibroblasts, iPSCs and hematopoietic cells derived from WAS-iPSCs (WASX503R-R#1). Peripheral blood mononuclear cells (PBMCs) expressing WASP were used as a control. (C) Phase contrast photomicrographs of ES-sacs generated from WT-iPSCs and WAS-iPSCs on day 14; magnification 4X and 10X. (D) Flow cytometry analysis of progenitor cells isolated from ES-sacs. $CD34^+ CD45^-$ hematopoietic progenitor cells were observed in all iPSC lines. (E) The colony forming cell number of hematopoietic progenitors generated from human ESCs (CUHES), WT-iPSCs and WAS-iPSCs

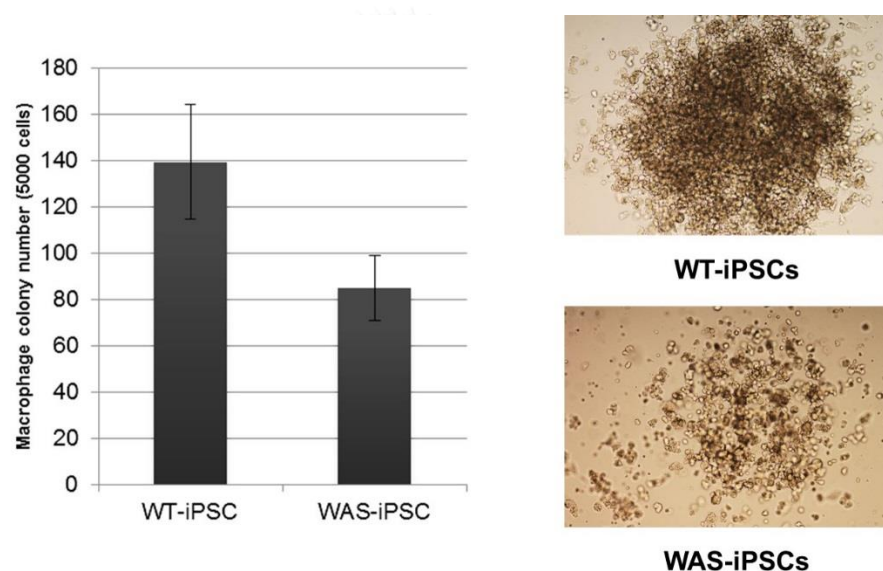


Figure 8 Hematopoietic progenitor cells generated from WAS-iPSCs showed defect in macrophage differentiation potential. Cells isolated from SAC were differentiated to macrophage using methycellulose media supplemented with M-CSF. The number and size of macrophage colony in WAS-iPSCs group were less than WT-iPSCs.

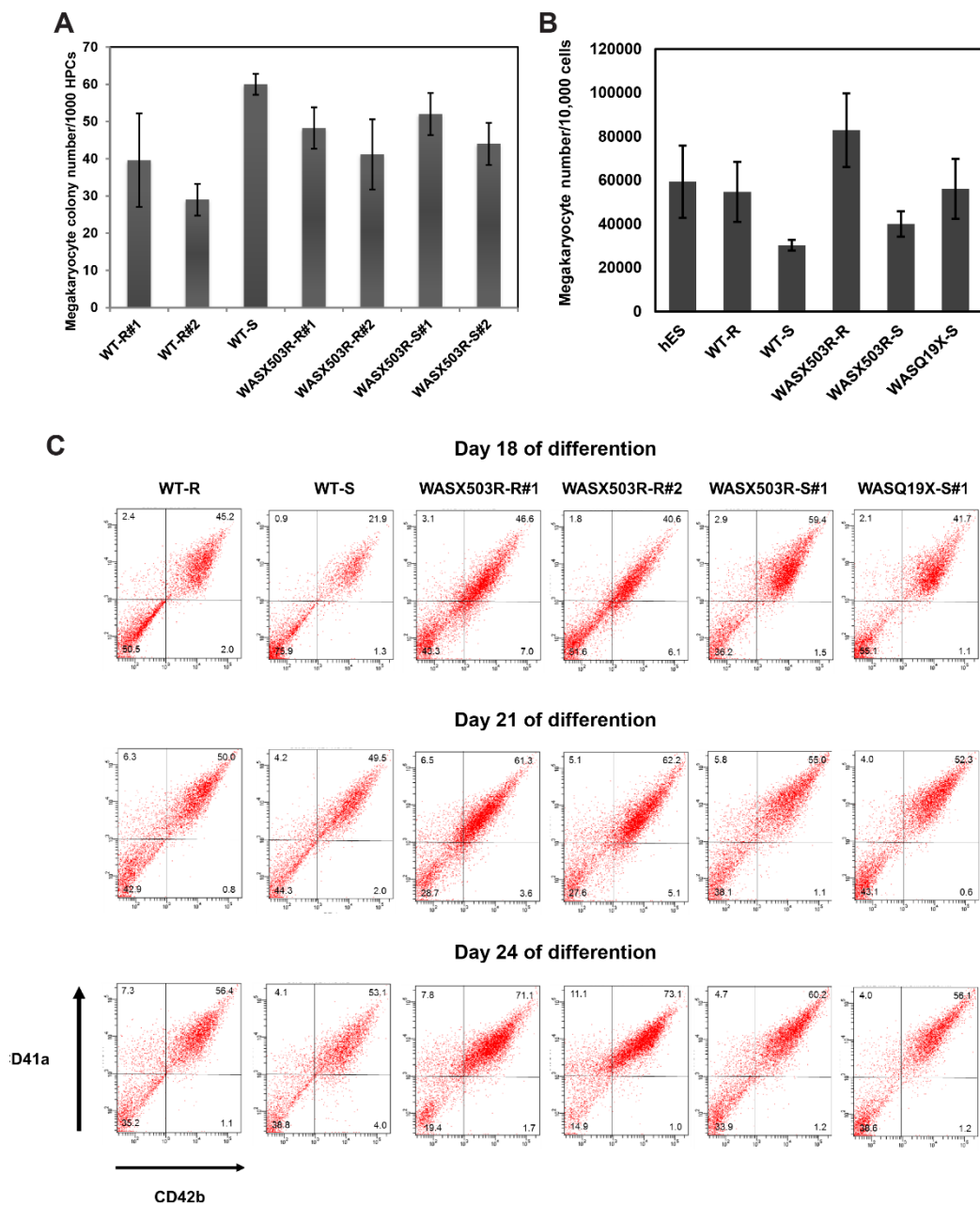


Figure 9 WT-iPSCs and WAS-iPSCs generated similar numbers of megakaryocytes (A) ES-sac derived HPCs on day 14 were cultured in Megacult media for 10 days. The resulting colonies were fixed, stained and counted. The number of megakaryocyte colonies observed in each group was not significantly different. Data were presented as mean \pm SEM, $n=4$. (B) 10,000 ES-sac derived HPCs on day 14 were cultured on mitotically inactivated OP9 feeder cells with megakaryocyte differentiation media. Bar graph showed the total number of CD41⁺ and CD42⁺ megakaryocytes derived from

hESCs, WT-R#1, WT-S, WASX503R-R#1, WASX503R-S#1 and WASQ19X-S#1. Data were presented as mean \pm SEM, $n=3$. (C) Flow cytometry analysis of megakaryocytes derived from WT-R, WT-S, WASX503R-R#1, WASX503R-R#2, WASX503R-S#1 and WASQ19X-S#1 on days 18, 21 and 24 using FITC-conjugated anti-human CD41 and PE-conjugated anti-human CD42b. There were higher percentages of megakaryocytes ($CD41^+/CD42b^+$) in cells differentiated from WASX503R-R#1, 2 on days 21 and 24 compared to other lines.

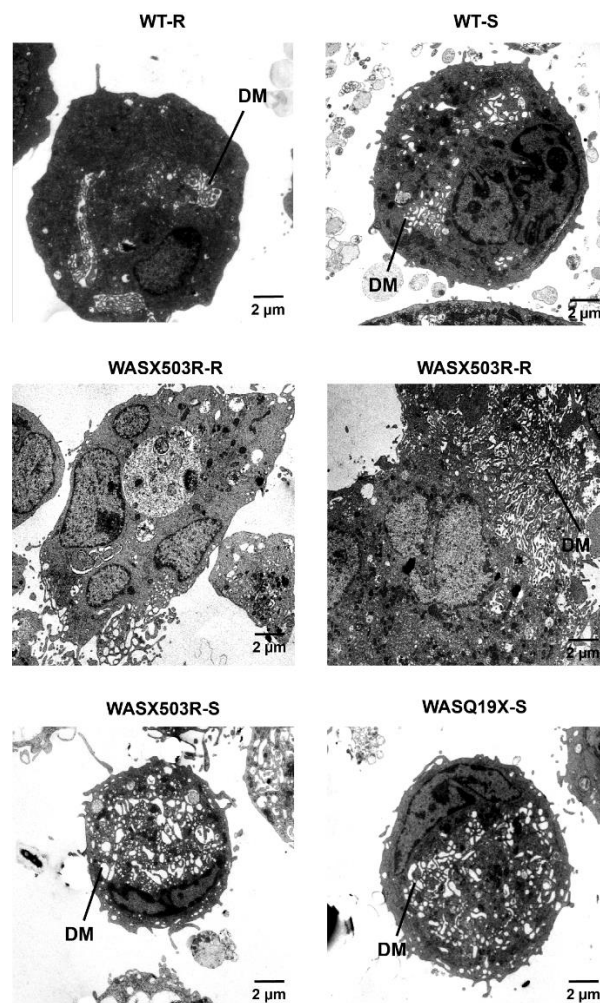


Figure 10 Megakaryocytes generated from WAS-iPSCs. Electron microscopic examination of megakaryocytes generated from WT-R#1, WT-S, WASX503R-R#1, WASX503R-S#1 and WASQ19X-S#1 derived megakaryocytes. Demarcation membrane system (DM) within the cytoplasm was observed in megakaryocytes derived from all iPSC lines. Notably, DM of megakaryocytes derived from WASX503R-R#1 was rarely observed. The abnormality of demarcation membrane system was seen as small-

sized fragments throughout the cytoplasm of megakaryocytes (left). WASX503R-R#1 derived megakaryocytes also demonstrated lower organelle contents within cytoplasm compared to the WT control (right).

Isogenic model and WASP overexpression rescued small size platelets

Previous studies using CD34⁺ cell from WAS patient showed that megakaryocytes generated from these cells cannot represent the platelet defects in vitro. We validated whether iPSC system could be used to model the microthrombocytopenia in WAS. Megakaryocyte culture supernatant at day 24 were collected and number of CD41+CD42b+ platelet-like particles were counted by using flow cytometry. FSC and SSC setting of peripheral blood platelet of healthy control were used for gating (Figure 11A). The number of platelet-like particles generated from WASQ19X#2, 3 and 4 were not different to those generated from hES, WT-R#1 and WT-S. Significant lower in platelet number were observed in WASX503R-R#1, 2, WASX503R-S#1, 2 and WASQ19X-S#1 (Figure 11B). Our data suggested that in vitro differentiation of iPSCs could not be used to model thrombocytopenia in WAS. Further investigation of platelet functional assay such as in vivo platelet consumption need to be performed.

To examine the platelet size and structure, platelets produced in megakaryocyte culture at day 24 were collected by multistep centrifugation. Platelet ultrastructure was analyzed by EM. We found that distribution of platelet granules was normal in all group except WASX503R-R#1 similar to their megakaryocytes (Figure 12A). Irregular shape and smaller size were observed in platelet-like particles generated from WAS groups. As measured under the electron microscope, diameter of platelet-like particle derived from WASX503R-S#1 (1.927 ± 0.934 um) and WASQ19X-S#1 (2.317 ± 0.951 um) was significantly smaller than WT-R#1 (3.234 ± 0.860 um) and WT-S (2.665 ± 0.852 um), respectively. To further quantitative analysis of platelet size, platelet pellet were spread on glass slide. Discoid shape platelets were stained with alpha-tubulin antibody and their diameter was measured under the fluorescence microscope

(Figure 12B). Consistence with EM data, tubulin coil diameter of platelets generated from WASX503R-S and WASQ19X-S were significantly smaller than the controls (Figure 12D). We next test whether the expression of WASP in hematopoietic progenitor cells derived from WAS-iPSCs could rescue the defect of the platelet size. WASQ19X-S derived hematopoietic progenitor cells were transduced with Lentiviral expressing WASP. Interestingly, mean platelet size generated from WASQ19X-S+WASP derived megakaryocytes was increased when compared to WASQ19X-S (Figure 12C and D).

Isogenic model which genetics are identically matched to the parental cells except the disease mutation, provide a better system for studying disease biology. In order to generate isogenic corrected WAS-iPSCs, WASX503R mutation specific ZFN and donor vector were designed as shown in Figure 13A. After nucleofection, corrected WASX503R-S iPSCs were selected and the correct modification at WASP locus was confirmed by DNA sequencing. To check whether WASP expression was restored, corrected WASX503R-S iPSCs were differentiated to hematopoietic cells and western blot was performed. Unfortunately, WASP were not detected in hematopoietic cells derived from corrected WASX503R-S iPSCs (Figure 13B). We hypothesized that insertion of selection cassette next to WASP stop codon might interfered protein expression. As expected, after cre recombinase mediated removal of selection cassette, WASP expression was shown in cre-corrected WASX503R-S iPSC derived hematopoietic cells. We next tested whether the restored WASP expression could rescued small size platelets. The mean size of cre-corrected WASX503R-S iPSC derived platelet as measured from tubulin coil diameter was increased compared to the parental line (Figure 14C and D). The isogenic, cre-corrected WASX503R-S iPSCs, strongly support the role of WASP in regulating platelet size. Thus, our result demonstrated that the WAS-iPSCs could recapitulated small size platelet which is the hallmark of WAS in vitro.

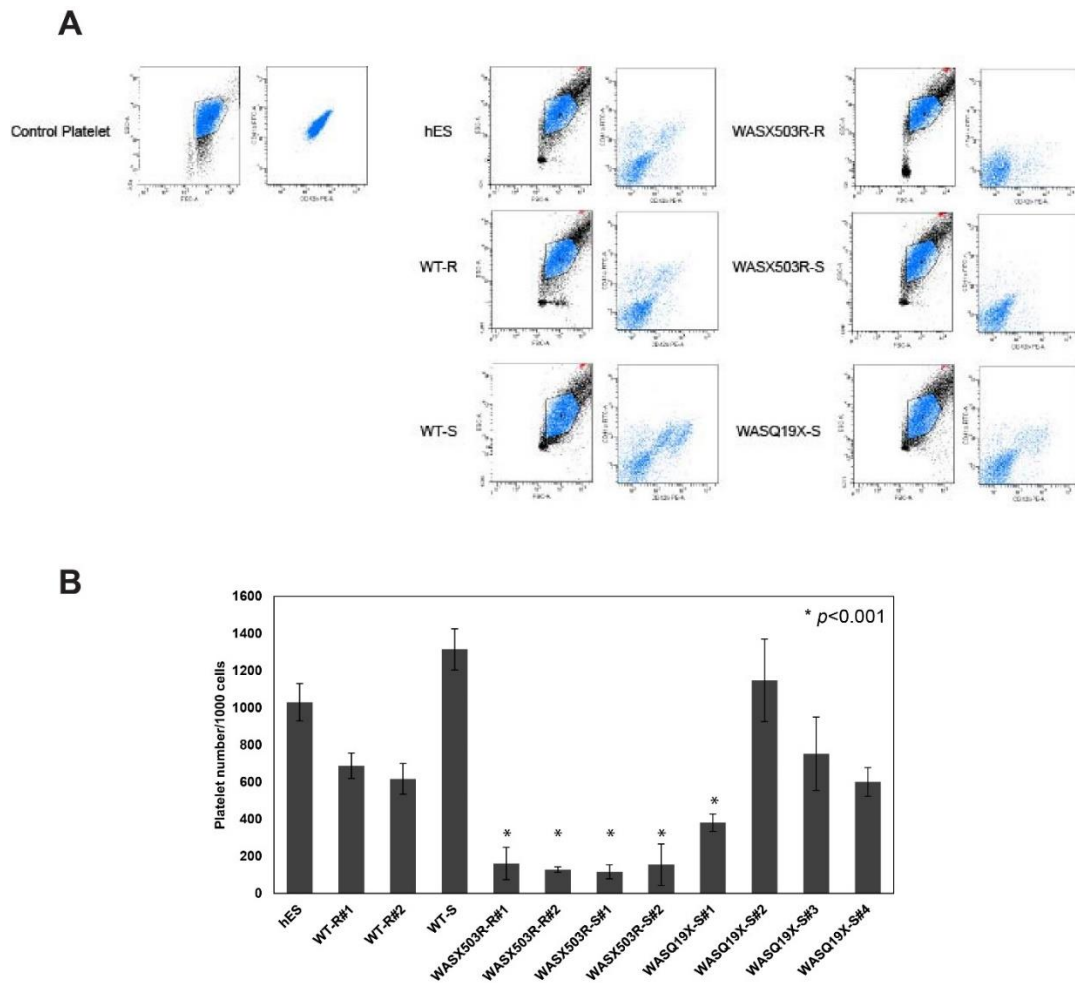


Figure 11 Flow cytometry analysis of platelet-like particle produced in cultured supernatant. Day24 of megakaryocyte differentiation, cultured supernatant were collected and stained with anti-CD41a FITC and CD42b-PE. (A) Platelet like particles were gated by using same FSC and SSC as normal platelets. Number of platelet like particles were counted by using CountBright™ absolute counting beads (Invitrogen). (B) Bar graph showing the number of platelet-like particles generated from hESCs, WT-R, WT-S, WASX503R-R, WASX503R-S and WASQ19X-S. Data are presented as mean \pm SEM, $n=5$. The asterisks (*) denote the results that are significantly different ($p<0.001$) from those obtained from the WT-iPSCs.

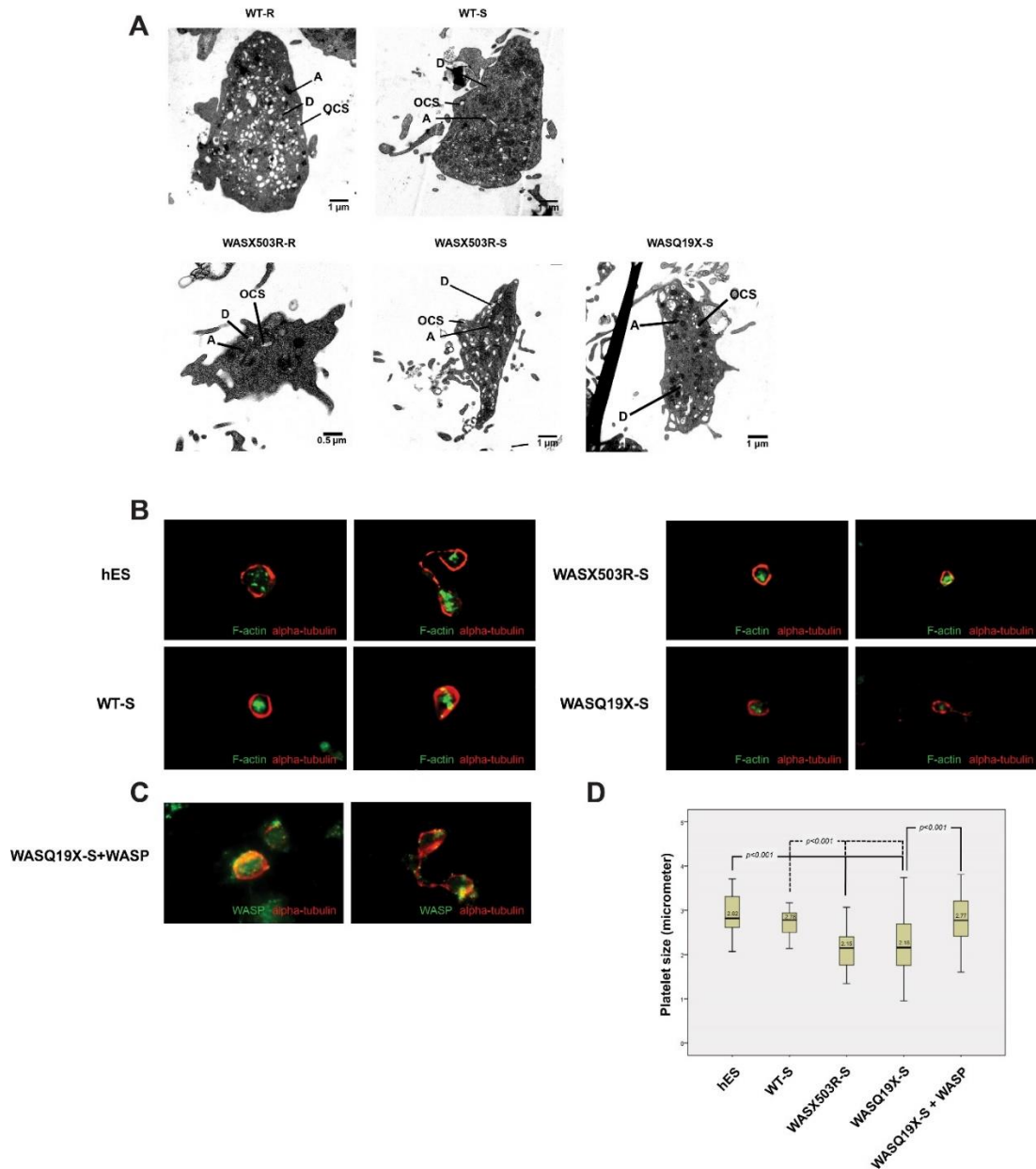


Figure 12 WAS-iPSCs produced small platelet size. (A) Transmission electron micrograph showing ultrastructure of platelet-like particles obtained from WT-R#1, WT-S, WASX503R-R#1, WASX503R-S#1 and WASQ19X-S#1. Platelet-like particles derived from WT-R#1, WT-S, WASX503R-S#1 and WASQ19X-S#1 demonstrated several organelles including dense body (D), alpha granule (A) and open canalicular system (OCS) throughout the cytoplasm of platelet-like particles. Platelet-like particles obtained from WASX503R-R#1 had non-discoid shapes with lower numbers of platelet organelles and granules. (B) Immunofluorescence staining of platelet particles

(magnification 100X). The platelet particles were stained with anti- α -tubulin (red) and phalloidin-FITC (green). (C) WASQ19X-WASP-derived platelets were stained with anti- α -tubulin (red) and anti-WASP (green). (D) A box plot showing the diameter of tubulin-stained discoid-shaped platelets generated from hESCs, WT-S, WASX503R-S#1, WASQ19X-S#1 and WASQ19X-S#1+WASP. Data are presented as mean \pm SEM, $n=31$. The asterisks (*) denote the results that are significantly different ($p<0.001$) from those obtained from the WT-iPSCs.

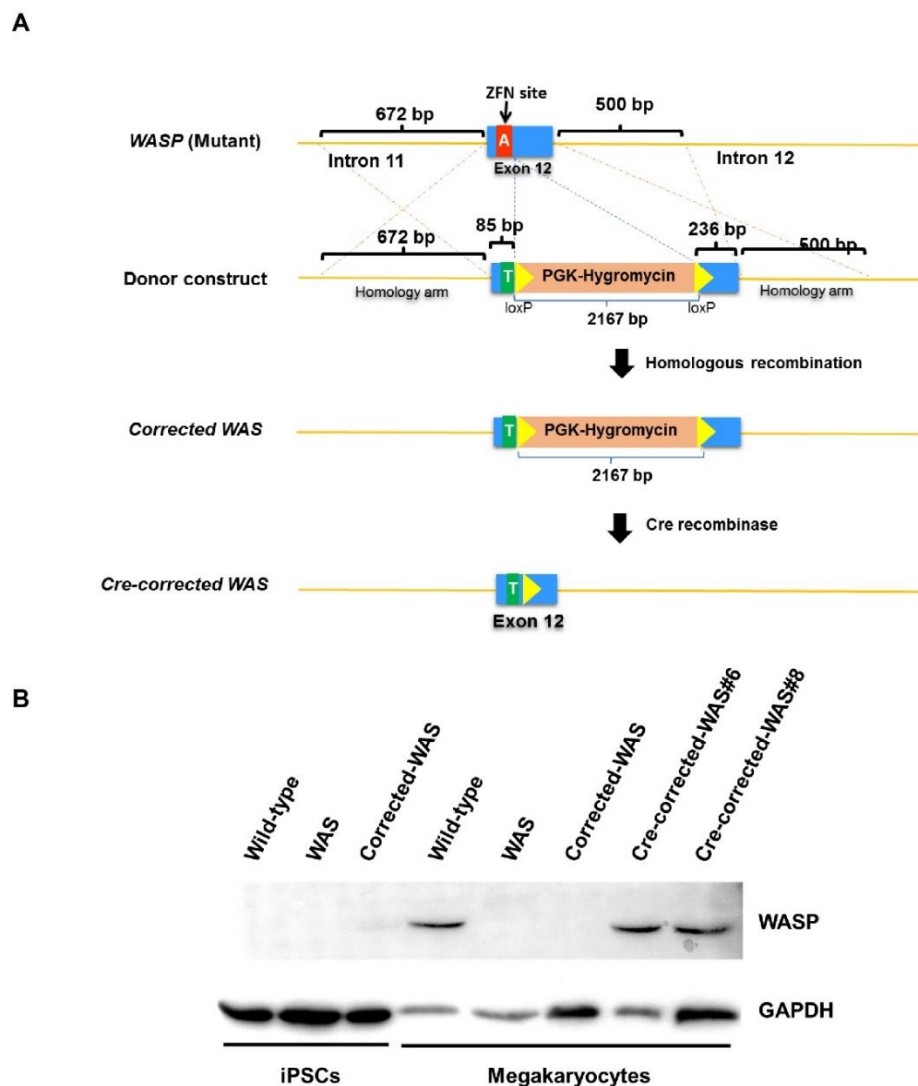


Figure 13 Genetic correction of WASP gene in WASX503R-S by using ZFN technology. (A) Schematic diagram of WASPX503R mutation correction. (B) Western

blot analysis showing WASP expression in hematopoietic cells derived from Cre-corrected WAS-iPSCs (WASX503R-S) but not corrected WAS-iPSCs.

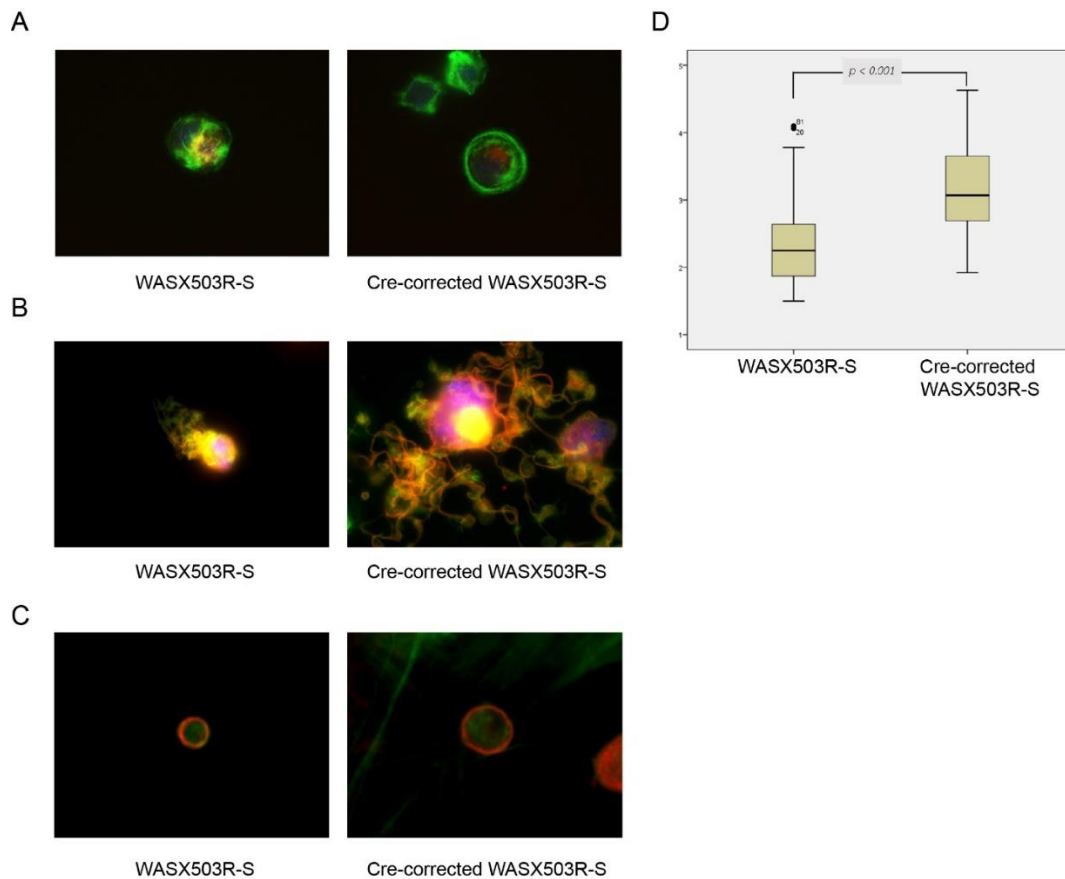
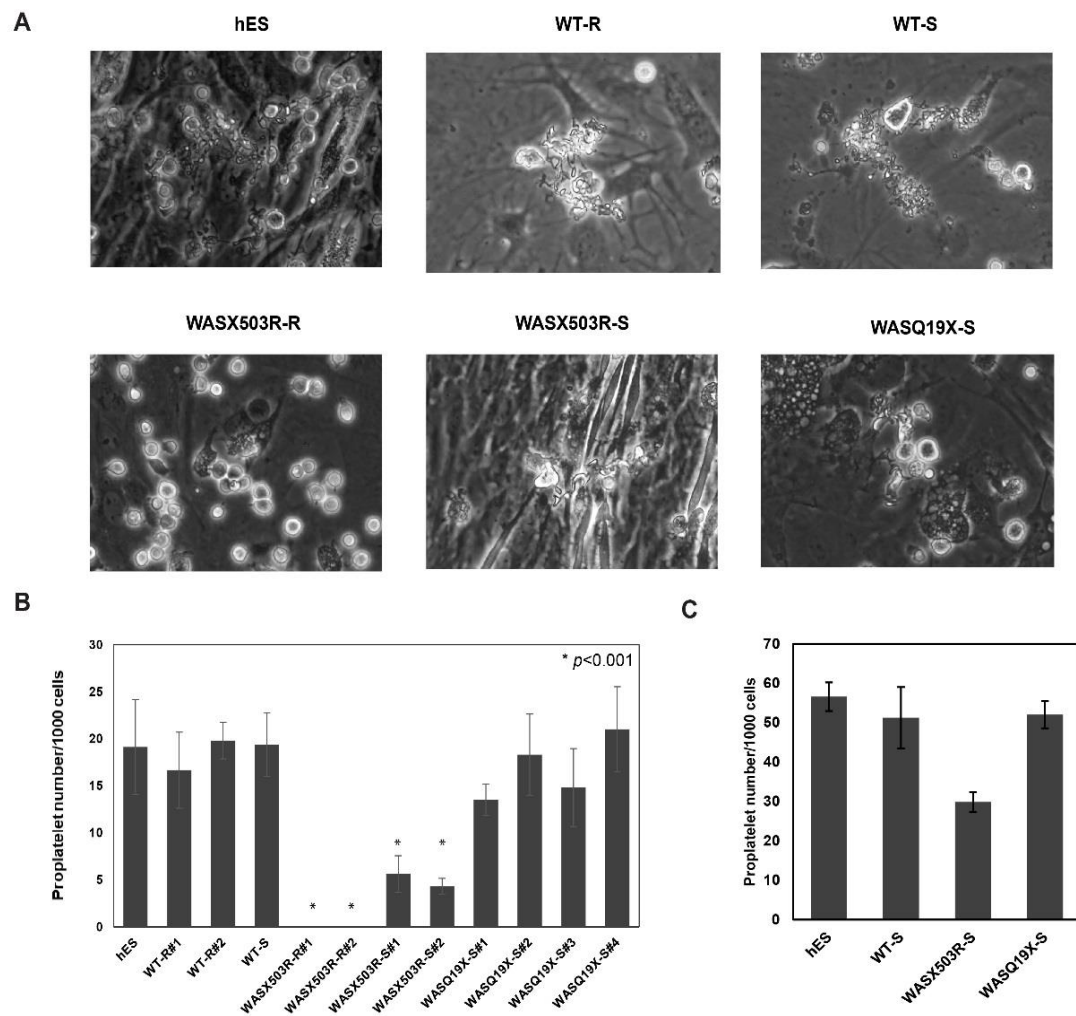


Figure 14 Restored WASP expression rescued the defects observed in WAS-iPSC derived megakaryocytes. Immunofluorescence staining of (A) megakaryocytes derived from WAS-iPSCs and Cre-corrected WAS-iPSCs using phalloidin-FITC (green) and anti CD42b-PE (red) after cultured on collagen I for 2 hr (B) proplatelet and (C) platelet-like particle derived from WAS-iPSCs and Cre-corrected WAS-iPSCs using phalloidin-FITC (green) and anti-alpha-tubulin (red) demonstrating that all the expression of WASP in WAS-iPSCs corrected the defects in F-actin polymerization, proplatelet formation and platelet size. DAPI (blue) was used for nuclear staining (magnification 100X).

Megakaryocytes derived from WAS-iPSCs exhibited defects in proplatelet formation.

It has been proposed that megakaryocytes released platelets into blood stream by extended long processes of its cytoplasm called proplatelet toward sinusoidal blood vessel of bone marrow. Spontaneous megakaryocytes elaborated proplatelet formation could be observed in culture of human and mouse derived cells. To further investigate whether WAS-iPSC derived megakaryocytes have defects in thrombopoiesis, proplatelets produced in megakaryocyte culture were analyzed. Long processes proplatelet cluster with numeral platelet buds were observed in hES, WT-R and WT-S derived megakaryocytes (Figure 15A). WASX503R-S and WASQ19X-S derived proplatelets exhibited shorter processes with abnormal platelet buds. Notably, proplatelet formation was not detected in WASX503R-R derived megakaryocytes. While proplatelet defect was observed in both WAS-X503R-S and WASQ19X-S, the reduction in proplatelet number was observed in WASX503R-S only (Figure 15B). Osteoblastic microenvironment has been shown to inhibit proplatelet formation both in vitro and in vivo. To investigate whether osteoprogenitor (OP9) feeder contribute to proplatelet defect observed in WAS-iPSC derived megakaryocytes. Megakaryocytes at day 21 of differentiation were isolated and reseeded on matrigel-coated plate and cultured for 24 hours. The number of proplatelet forming cells were counted and proplatelet structure were analyzed by staining with alpha-tubulin antibody. The number of proplatelet formation in all groups were increased compared with feeder system (Figure 15C). However, the number of proplatelet generated from WASX503R-s still lower. Interestingly, proplatelet derived from WASX503R-s and WASQ19X-S exhibited thin proplatelet shafts, less branching and small platelet buds at the end of proplatelet tips (Figure 15D). Thickness of proplatelet shaft extended from WASP overexpressed WASQ19X and cre-corrected WASX503R-S derived megakaryocytes were remarkably increased and showed more branching (Figure 14B and 15E). Size of platelet buds at the end of proplatelet tips also increased which correlated with the bigger mean

platelet size. These data suggested the role of WASP in controlling proplatelet formation and regulating platelet size. In addition, we also showed that OP9 feeder cells, in part, has an effect on the number of proplatelet formation. Our in vitro differentiation system could be used to model other platelet disease (Figure 16).



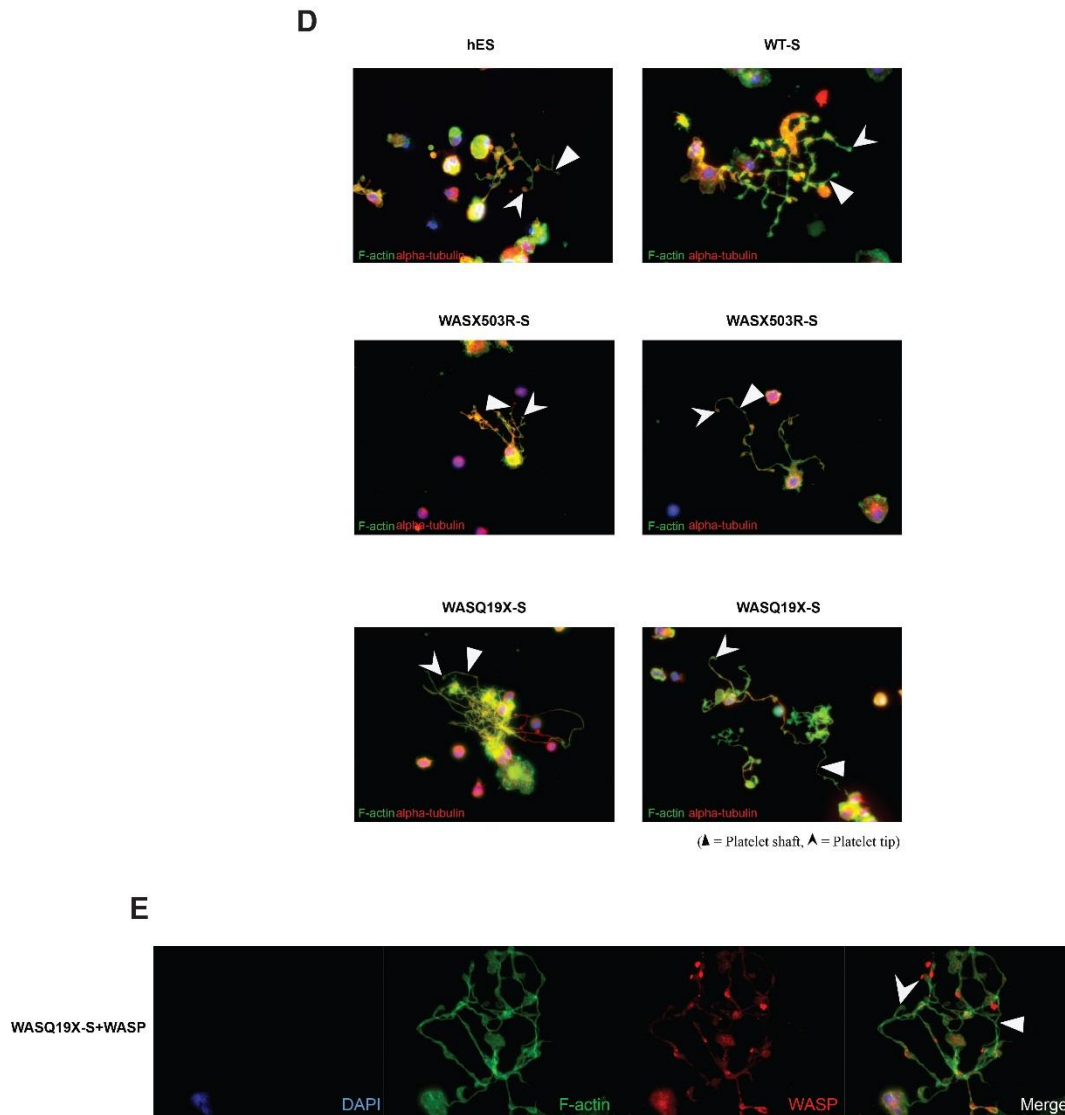


Figure 15 *WAS-iPSC-derived megakaryocytes showed abnormal proplatelet structures.* (A) Phase contrast images of megakaryocytes derived from hESCs, WT-R#1, WT-S, WASX503R-R#1, WASX503R-S#1 and WASQ19X-S#1. Proplatelet formation was detected in hESCs, WT-R#1, WT-S, WASX503R-S#1 and WASQ19X-S#1 derived megakaryocytes. Proplatelet arm extension of WASX503R-S#1 and WASQ19X-S#1 derived megakaryocytes was shorter than that of the WT group. (B) On day 21 of differentiation, 1000 iPSC-derived megakaryocytes were reseeded on mitotically inactivated OP9 feeder cells. The number of proplatelet forming cells was counted on day 22. Data are presented as mean \pm SEM, n=5. Proplatelet forming cells were detected in the hESCs, WT-R, WT-S, WASX503R-S and WASQ19X-S derived megakaryocytes while they were undetectable at any time point in the WASX503R-R.

(C) 1000 iPSC-derived megakaryocytes were reseeded on the matrigel coated plate. The number of proplatelet forming cells was counted on day 22. Data were presented as mean \pm SEM, n=5. The number of proplatelet forming cells detected in hESCs, WT-S, WASX503R-S#1 and WASQ19X-S#1 derived megakaryocytes were higher compared to that in cells cultured in the OP9 feeder condition. iPSC-derived megakaryocytes were reseeded on matrigel coated cover slides and cultured for 24 hours. Proplatelet forming cells were fixed and stained with anti- α -tubulin (red) and phalloidin-FITC (green). (D) WASX503R-S#1 and WASQ19X-S#1 derived megakaryocytes showed abnormal proplatelet structures with small-sized platelet particles at the end of the proplatelet tip compared to the WT control (magnification 40X). (E) WASQ19X-S#1 derived megakaryocytes were transduced with lentiviruses expressing WASP (WASQ19X-S#1+WASP).

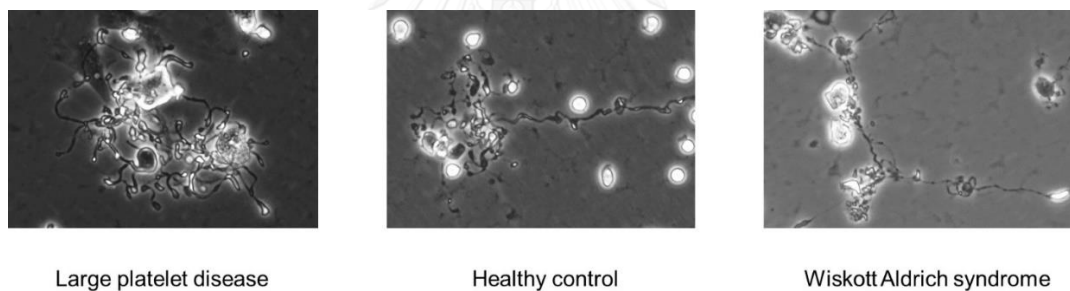


Figure 16 *in vitro* iPSCs differentiation for modeling large platelet disease. Megakaryocytes generated from large platelet disease iPSCs showed thick proplatelet shaft with large size platelet buds.

WAS-iPSC derived megakaryocyte showed defect in actin reorganization

WASP functions as a regulator of actin polymerization. Megakaryocytes from WASP-deficient mice exhibited defect in F-actin spreading and assembly. In order to test the F-actin reorganization, megakaryocytes derived from iPSCs were cultured on Collagen I-coated slide for 2 hours. Whereas periphery actin polymerization was observed in WT-iPSC derived megakaryocytes, abnormal distribution of F-actin throughout

cytoplasm was detected in WAS-iPSC derived megakaryocytes (Figure 17). Restoration of WASP expression in cre-corrected WASX503R-S, actin polymerization at the periphery of megakaryocyte cytoplasm were detected (Figure 14A). Our data support the role of WASP in actin reorganization of hematopoietic cells. All these data demonstrated that the in vitro differentiation of iPSCs could recapitulate abnormalities in thrombopoiesis observed in WAS.

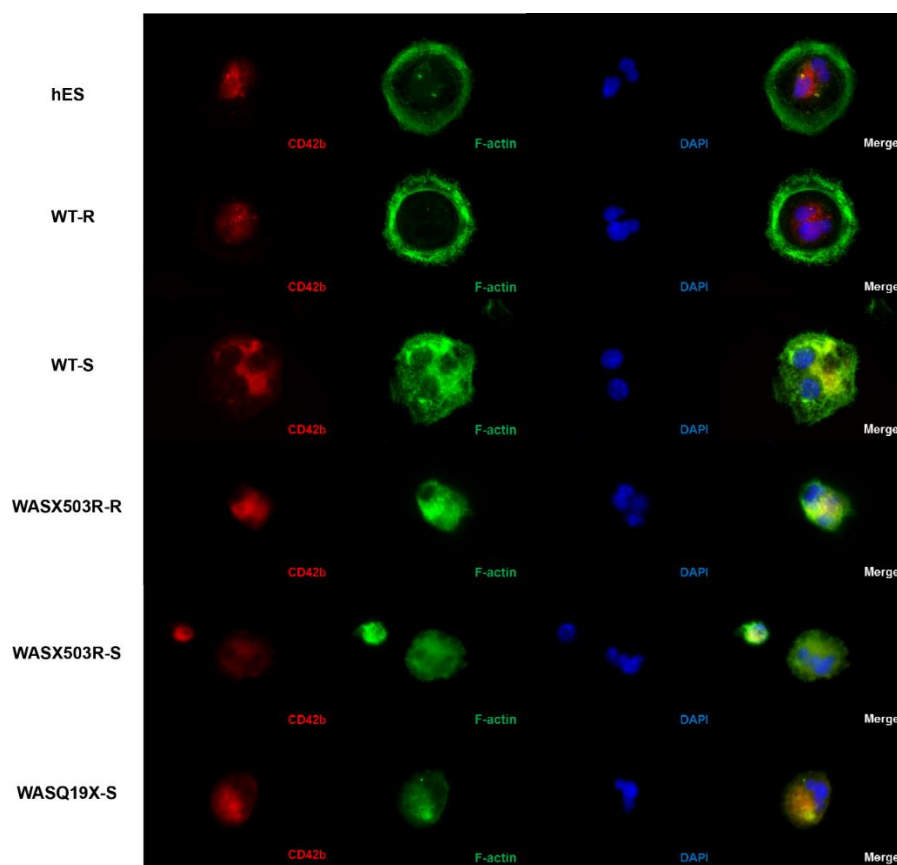


Figure 17 Cytoskeleton reorganization in megakaryocytes derived from WAS-iPSCs. Immunofluorescence staining of megakaryocytes derived from hESCs, WT-R#1, WT-S, WASX503R-R#1, WASX503R-S#1 and WASQ19X-S#1 using phalloidin-FITC (green) and anti CD42b-PE (red) demonstrating that all WT-iPSC-derived megakaryocytes retained normal actin polymerization. DAPI (blue) was used for nuclear staining (magnification 100X).

Xenotransplantation of iPSC derived CD34⁺ cells showed lymphoid engraftment

Cre-corrected WASX503R-S iPSC can be used as a cell source for generating long-term engraftable HSCs for cell replacement therapy. Nonetheless, xenotransplantation of CD34⁺ cells derived from iPSCs, could not well engrafted as the human cell chimerism were rarely detected in mouse peripheral blood after transplantation. Most of the engrafted cells were CD15⁺ CD45⁺ monocytes, CD3⁺ and CD19⁺ cells were hardly detected. In order to improve engraftment and reconstitution potential of iPSC derived HSCs, we optimized method for purification and transplantation of iPSC derived CD34⁺ cells. Sixteen months after transplantation, importantly, multilineage engraftment and detection of myeloid and lymphoid cells were observed in WT-S, WASX503R-S and Cre-corrected WASX503R-S (Figure 18). Notably, the reconstitution activity of CD34⁺ cell derived from WASX503R-S seem to be lower than the others. These data suggested the role of WASP in HSC engraftment.

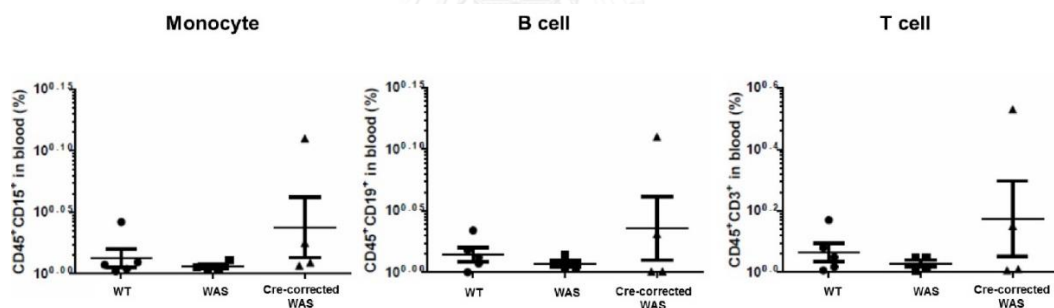


Figure 18 Transplantation of iPSC derived CD34⁺ HPCs into humanized mice showed T cell engraftment. After 16 months of transplantation, human CD15⁺CD45⁺ (monocytes), CD19⁺CD45⁺ (B cells) and CD3⁺CD45⁺ (T cells) were detected in mouse peripheral blood.

CHAPTER V

DISCUSSION

Although human hematopoietic stem cells and megakaryocytes can be readily obtained from various sources, without effective methods for long-term *in vitro* expansion and genetic manipulation, it has been difficult to study the function of human genes involved in platelet biogenesis. Many established inherited thrombocytopenia mouse models fail to recapitulate platelet defects due to the different between mouse and human biology (Alexander, Roberts et al. 1996; Boulet and Capecchi 2004; Albers, Paul et al. 2012). Induced pluripotent stem cells (iPSCs), generated by epigenetic reprogramming of somatic cells of patient with inherited platelet disorders, provide a potential invaluable tool for elucidating molecular mechanism of rare human genetic disease *in vitro*. Nevertheless, previously there were only a few reports describing *in vitro* platelet production using human pluripotent stem cells (Takayama, Nishikii et al. 2008; Lu, Li et al. 2011). Due to confounding factors, such as the reprogramming process, the complexity of the *in vitro* differentiation methods, and the lack of bone marrow microenvironment factors, it has been unclear whether platelet produced from patient-specific iPSCs could exhibit disease phenotype especially micro- and macrothrombocytopenia *in vitro*. In this study we comprehensively examined the strengths and limitations of using iPSCs combining with genome editing techniques in modeling platelet disorders including Wiskott-aldrich syndrome and Bernard-Soulier-like syndrome.

The cellular and molecular basis of the process control platelet size is poorly understood. In contrast to microthrombocytopenia invariably observed in WAS patients, murine models of WASP deficiency exhibited only mild thrombocytopenia with normal-sized platelets (Sabri, Foudi et al. 2006). Platelet size has been proposed to regulate by both intrinsic and extrinsic factors including sheer force (Thon, Montalvo

et al. 2010) and bone marrow environment (Deutsch and Tomer 2013) which potentially limits the ability to model platelet size defect in vitro. Because all of our WAS-iPSC lines produced platelets that are smaller than control in the culture system without shear force, and increase level of WASP expression using lentivirus or ZFN-mediated gene editing increase platelet size compared to uncorrected isogenic lines, our findings suggest that WASP levels play a substantial role in determining platelet size. For hereditary macrothrombocytopenia, we demonstrated that iPSCs generated from fibroblasts of a patient with unknown familial macrothrombocytopenia faithfully produced large-size platelets in our system. The reproducibility of the system validates its use for modeling human genetic disease affecting platelet biogenesis.

The defective in proplatelet production of WAS derived megakaryocytes still controversies, There was a report that CD34⁺ cells isolated from WAS patients exhibited normal proplatelet formation (Haddad, Cramer et al. 1999). Our in vitro model allowed us to closely observe the proplatelet processes. We observed small size platelet buds at the end of proplatelet processes of the WAS-iPSC derived MKs. Our findings are consistent with the fact that microtubule coil diameter of and thickness at platelet buds has been shown to be associated with terminal platelet size (Thon and Italiano 2012; Thon, Macleod et al. 2012). Abnormally thin, less branching proplatelet processes of WAS-iPSC derived megakaryocytes were similar to those observed in megakaryocytes treated with cytochalasin B and D, which prevent actin polymerization (Italiano, Lecine et al. 1999). Actin polymerization is known to promote bending and branching of proplatelet shaft that increase the number of proplatelet end which platelet are thought to release. Importantly, we demonstrate for the first time that an increase in WASP expression reverses the defects in proplatelet morphology and increases the size of the platelets. Taken together our data provide the evidence that WASP level is crucial for proplatelet formation likely through its effects on actin cytoskeleton.

While our system clearly demonstrates qualitative defects in platelet production, 3 out of 6 WAS-iPSCs produced comparable number of platelet-like particle to WT control. This finding suggested that the amount of platelet-like particle counted in our assay may not directly reflect degree of thrombocytopenia observed in the WAS patients. This may be due to the differences between our in vitro model and in vivo environment. In the bone marrow, megakaryocytes need to extend proplatelet processes through extracellular matrix into the sinusoidal blood vessels before shedding platelets (Patel, Hartwig et al. 2005). It is possible that the short, fragile proplatelet processes of WAS-MKs may not be able to reach blood vessels. Moreover, we observed a defect of F-actin localization in WAS-iPSC derived megakaryocytes after contacted with collagen, a major ECM in the bone marrow. Peripheral F-actin polymerization under the cell membrane of MKs has been proposed to prevent premature proplatelet formation within the bone marrow (Tablin, Castro et al. 1990). Taken together our data suggest the model that in the absent of WASP, MKs prematurely produces abnormal proplatelets that breakdown and release platelets within the bone marrow similar to what observed in WASP deficient mice (Sabri, Foudi et al. 2006). The molecular mechanism by which WASP participated in regulating cytoskeleton during platelet formation will be further studied by using WASP-GFP and MK-specific promoter driven actin reporter iPSC lines we already created with genome editing techniques. On the other hand, accelerated platelet destruction could also contribute to low platelet count in WAS patient (Prislovsky and Strom 2013; Prislovsky, Zeng et al. 2013). Splenectomy has been shown to increase platelet count in many WAS patients (Lum, Tubergen et al. 1980). It is possible that the thin tubulin coil, irregular shape platelets, produced from WAS-iPS derived MKs, may exhibit shorter half-life than control in vivo. Further study using in vivo platelet consumption will be required in order to solve this issue. Although our model could not accurately predict the severity of thrombocytopenia, it still provide a viable platform for screening effective drugs, small molecules, and gene therapy strategy for improving platelet production in WAS and other platelet disorders.

We demonstrated that the methods used for iPSC generation could affect its reliability for disease modeling. Megakaryocytes and platelets derived from iPSCs produced with retrovirus method from showed more pronounced defects than those produced with sendai virus. This is probably caused by reactivation of integrated transgene during cell differentiation. All Yamanaka's factors by itself can affect various cell properties. Integrating vectors could also disrupt important gene or regulatory sequences. Therefore, even in disease modeling, newer non-integrating methods such as sendai viruses, mRNA or episomes are preferred. The issue of heterogeneity among different iPSC lines can be addressed with gene-engineered/corrected isogenic lines. In our study we showed that antibiotic selection cassette at the site near corrected WASP gene could interfere with WASP expression and cell behavior. Thus, selection cassette removal strategy should be included in the donor vector design.

Abnormal bleeding and immune deficiency are leading causes of death in patients with severe WAS. Restoring immune cell functions normally requires allogeneic hematopoietic stem cell transplantation, the only curative therapy for WAS. The difficulty in finding HLA-matched donors and complications related to transplantation urge the development of gene therapy strategies for WAS. Hematopoietic stem cell gene therapy using retroviral and lentiviral vectors has shown to restore natural killer, T and B cell functions both in mouse models (Bosticardo, Draghici et al. 2011; Astrakhan, Sather et al. 2012) and in patients with WAS. (Boztug, Schmidt et al. 2010; Aiuti, Biasco et al. 2013; Braun, Boztug et al. 2014; Hacein-Bey Abina, Gaspar et al. 2015) Nevertheless, most of the patients from the clinical trials subsequently developed T cell leukemia, potentially caused by vector integration at the T-cell oncogene, LMO2 site.(Galy and Thrasher 2011) Therefore, the issues of random integration, appropriate viral vector design, optimal levels of WASP expression in each hematopoietic lineage, and prevention of transgene silencing need to be solved before it could become a safer and more effective therapy. Recent study, the integration of gp91^{phox} into AAVS1 site of iPSCs from X-linked chronic granulomatous

patients by using ZFN corrected the function of neutrophils similar to that use self-inactivating lentiviral vectors containing gp91^{phox} (Zou, Sweeney et al. 2011). In contrast to gene therapy, insertion in to precise genome location provide a safer method. We are in the process of evaluating the effects between ZFN targeting at AAVS1 site and ZFN mediated site specific gene correction.

Site specific genome editing of single mutation in patient specific iPSCs by homologous recombination using nuclease technology has been proposed as the alternative way to generate corrected hematopoietic stem cells for curative hematological diseases. Transplantation of genetically corrected iPSC derived hematopoietic progenitor cells could corrected sickle cell anemia phenotype in mouse (Hanna, Wernig et al. 2007), proved the concept of using corrected iPSCs for future cell replacement therapy. In this study, we demonstrated the restore WASP expression by genome editing using ZFN could rescued the platelet defects in WAS-iPSCs, indicated the potential of these cells to be used for autologous transplantation. However, the safety and function of iPSC derived hematopoietic cells need to be addressed before clinical translation. Xenotransplantation of hematopoietic progenitor cells derived from iPSCs showed low engraftment in humanized mice recipients (Ledran, Krassowska et al. 2008; Risueno, Sachlos et al. 2012; Doulatov, Vo et al. 2013). This issue has hampered clinical application of iPSC derived hematopoietic progenitors cells and suggests that these cells require additional cues for definitive hematopoiesis. There are many group attempted to develop differentiation protocol the drive definite hematopoietic cell fate (Amabile, Welner et al. 2013; Amabile, Welner et al. 2013; Suzuki, Yamazaki et al. 2013). With the improvement of purification and transplantation protocols, multilineage engraftment including monocytes, T cell and B cells were observed in our recipient mice. Their long-term engraftment potential need to be tested by serial transplantation. With the improvement in techniques for generating engraftable long term hematopoietic stem cells and advances in gene targeting strategies, gene

corrected hematopoietic stem cells generated from patient iPSCs may one day a viable alternative treatment for hematological diseases.



REFERENCES

- Aiuti, A., L. Biasco, et al. (2013). "Lentiviral hematopoietic stem cell gene therapy in patients with Wiskott-Aldrich syndrome." *Science* **341**(6148): 1233-1235.
- Albers, C. A., D. S. Paul, et al. (2012). "Compound inheritance of a low-frequency regulatory SNP and a rare null mutation in exon-junction complex subunit RBM8A causes TAR syndrome." *Nat Genet* **44**(4): 435-439, S431-432.
- Albert, M. H., T. C. Bittner, et al. (2010). "X-linked thrombocytopenia (XLT) due to WAS mutations: clinical characteristics, long-term outcome, and treatment options." *Blood* **115**(16): 3231-3238.
- Aldrich, R. A., A. G. Steinberg, et al. (1954). "Pedigree demonstrating a sex-linked recessive condition characterized by draining ears, eczematoid dermatitis and bloody diarrhea." *Pediatrics* **13**(2): 133-139.
- Alexander, W. S., A. W. Roberts, et al. (1996). "Deficiencies in progenitor cells of multiple hematopoietic lineages and defective megakaryocytopoiesis in mice lacking the thrombopoietic receptor c-Mpl." *Blood* **87**(6): 2162-2170.
- Amabile, G., R. S. Welner, et al. (2013). "In vivo generation of transplantable human hematopoietic cells from induced pluripotent stem cells." *Blood* **121**(8): 1255-1264.
- Amarinthukrowh, P., S. Ittiporn, et al. (2013). "Clinical and molecular characterization of Thai patients with Wiskott-Aldrich syndrome." *Scand J Immunol* **77**(1): 69-74.
- Astrakhan, A., B. D. Sather, et al. (2012). "Ubiquitous high-level gene expression in hematopoietic lineages provides effective lentiviral gene therapy of murine Wiskott-Aldrich syndrome." *Blood* **119**(19): 4395-4407.
- Ban, H., N. Nishishita, et al. (2011). "Efficient generation of transgene-free human induced pluripotent stem cells (iPSCs) by temperature-sensitive Sendai virus vectors." *Proc Natl Acad Sci U S A* **108**(34): 14234-14239.

- Bear, J. E., J. F. Rawls, et al. (1998). "SCAR, a WASP-related protein, isolated as a suppressor of receptor defects in late Dictyostelium development." J Cell Biol **142**(5): 1325-1335.
- Bosticardo, M., E. Draghici, et al. (2011). "Lentiviral-mediated gene therapy leads to improvement of B-cell functionality in a murine model of Wiskott-Aldrich syndrome." J Allergy Clin Immunol **127**(6): 1376-1384 e1375.
- Bosticardo, M., F. Marangoni, et al. (2009). "Recent advances in understanding the pathophysiology of Wiskott-Aldrich syndrome." Blood **113**(25): 6288-6295.
- Boulet, A. M. and M. R. Capecchi (2004). "Multiple roles of Hoxa11 and Hoxd11 in the formation of the mammalian forelimb zeugopod." Development **131**(2): 299-309.
- Boztug, K., M. Schmidt, et al. (2010). "Stem-cell gene therapy for the Wiskott-Aldrich syndrome." N Engl J Med **363**(20): 1918-1927.
- Braun, C. J., K. Boztug, et al. (2014). "Gene therapy for Wiskott-Aldrich syndrome--long-term efficacy and genotoxicity." Sci Transl Med **6**(227): 227ra233.
- Campellone, K. G., N. J. Webb, et al. (2008). "WHAMM is an Arp2/3 complex activator that binds microtubules and functions in ER to Golgi transport." Cell **134**(1): 148-161.
- Chatchatee, P., C. Srichomthong, et al. (2003). "A novel termination codon mutation of the WAS gene in a Thai family with Wiskott-Aldrich syndrome." Int J Mol Med **12**(6): 939-941.
- Derry, J. M., H. D. Ochs, et al. (1994). "Isolation of a novel gene mutated in Wiskott-Aldrich syndrome." Cell **79**(5): following 922.
- Deutsch, V. R. and A. Tomer (2013). "Advances in megakaryocytopoiesis and thrombopoiesis: from bench to bedside." Br J Haematol **161**(6): 778-793.
- Devriendt, K., A. S. Kim, et al. (2001). "Constitutively activating mutation in WASP causes X-linked severe congenital neutropenia." Nat Genet **27**(3): 313-317.
- Doulatov, S., L. T. Vo, et al. (2013). "Induction of multipotential hematopoietic progenitors from human pluripotent stem cells via respecification of lineage-restricted precursors." Cell Stem Cell **13**(4): 459-470.

- Dupre, L., A. Aiuti, et al. (2002). "Wiskott-Aldrich syndrome protein regulates lipid raft dynamics during immunological synapse formation." *Immunity* **17**(2): 157-166.
- Freson, K., R. De Vos, et al. (2005). "The TUBB1 Q43P functional polymorphism reduces the risk of cardiovascular disease in men by modulating platelet function and structure." *Blood* **106**(7): 2356-2362.
- Fusaki, N., H. Ban, et al. (2009). "Efficient induction of transgene-free human pluripotent stem cells using a vector based on Sendai virus, an RNA virus that does not integrate into the host genome." *Proc Jpn Acad Ser B Phys Biol Sci* **85**(8): 348-362.
- Galy, A. and A. J. Thrasher (2011). "Gene therapy for the Wiskott-Aldrich syndrome." *Curr Opin Allergy Clin Immunol* **11**(6): 545-550.
- Hacein-Bey-Abina, S., F. Le Deist, et al. (2002). "Sustained correction of X-linked severe combined immunodeficiency by ex vivo gene therapy." *N Engl J Med* **346**(16): 1185-1193.
- Hacein-Bey Abina, S., H. B. Gaspar, et al. (2015). "Outcomes following gene therapy in patients with severe Wiskott-Aldrich syndrome." *JAMA* **313**(15): 1550-1563.
- Haddad, E., E. Cramer, et al. (1999). "The thrombocytopenia of Wiskott Aldrich syndrome is not related to a defect in proplatelet formation." *Blood* **94**(2): 509-518.
- Hanna, J., M. Wernig, et al. (2007). "Treatment of sickle cell anemia mouse model with iPS cells generated from autologous skin." *Science* **318**(5858): 1920-1923.
- Hiroyama, T., K. Miharada, et al. (2008). "Establishment of mouse embryonic stem cell-derived erythroid progenitor cell lines able to produce functional red blood cells." *PLoS One* **3**(2): e1544.
- Inoue, H., N. Nagata, et al. (2014). "iPS cells: a game changer for future medicine." *EMBO J* **33**(5): 409-417.
- Italiano, J. E., Jr., P. Lecine, et al. (1999). "Blood platelets are assembled principally at the ends of proplatelet processes produced by differentiated megakaryocytes." *J Cell Biol* **147**(6): 1299-1312.

- Kajiwara, M., S. Nonoyama, et al. (1999). "WASP is involved in proliferation and differentiation of human haemopoietic progenitors in vitro." Br J Haematol **107**(2): 254-262.
- Kim, A. S., L. T. Kakalis, et al. (2000). "Autoinhibition and activation mechanisms of the Wiskott-Aldrich syndrome protein." Nature **404**(6774): 151-158.
- Kim, H. S., J. M. Bernitz, et al. (2014). "Genomic editing tools to model human diseases with isogenic pluripotent stem cells." Stem Cells Dev **23**(22): 2673-2686.
- Kim, K., A. Doi, et al. (2010). "Epigenetic memory in induced pluripotent stem cells." Nature **467**(7313): 285-290.
- Ledran, M. H., A. Krassowska, et al. (2008). "Efficient hematopoietic differentiation of human embryonic stem cells on stromal cells derived from hematopoietic niches." Cell Stem Cell **3**(1): 85-98.
- Lee, G., E. P. Papapetrou, et al. (2009). "Modelling pathogenesis and treatment of familial dysautonomia using patient-specific iPSCs." Nature **461**(7262): 402-406.
- Linardopoulou, E. V., S. S. Parghi, et al. (2007). "Human subtelomeric WASH genes encode a new subclass of the WASP family." PLoS Genet **3**(12): e237.
- Lu, S. J., F. Li, et al. (2011). "Platelets generated from human embryonic stem cells are functional in vitro and in the microcirculation of living mice." Cell Res **21**(3): 530-545.
- Lum, L. G., D. G. Tubergen, et al. (1980). "Splenectomy in the management of the thrombocytopenia of the Wiskott-Aldrich syndrome." N Engl J Med **302**(16): 892-896.
- Maeder, M. L., S. Thibodeau-Beganny, et al. (2008). "Rapid "open-source" engineering of customized zinc-finger nucleases for highly efficient gene modification." Mol Cell **31**(2): 294-301.
- Mali, P., L. Yang, et al. (2013). "RNA-guided human genome engineering via Cas9." Science **339**(6121): 823-826.
- Marchetto, M. C., C. Carromeu, et al. (2010). "A model for neural development and treatment of Rett syndrome using human induced pluripotent stem cells." Cell **143**(4): 527-539.

- Miharada, K., T. Hiroyama, et al. (2006). "Efficient enucleation of erythroblasts differentiated in vitro from hematopoietic stem and progenitor cells." Nat Biotechnol **24**(10): 1255-1256.
- Miki, H., K. Miura, et al. (1996). "N-WASP, a novel actin-depolymerizing protein, regulates the cortical cytoskeletal rearrangement in a PIP2-dependent manner downstream of tyrosine kinases." EMBO J **15**(19): 5326-5335.
- Miki, H., S. Suetsugu, et al. (1998). "WAVE, a novel WASP-family protein involved in actin reorganization induced by Rac." EMBO J **17**(23): 6932-6941.
- Miller, J. C., S. Tan, et al. (2011). "A TALE nuclease architecture for efficient genome editing." Nat Biotechnol **29**(2): 143-148.
- Molina, I. J., J. Sancho, et al. (1993). "T cells of patients with the Wiskott-Aldrich syndrome have a restricted defect in proliferative responses." J Immunol **151**(8): 4383-4390.
- Moretti, A., M. Bellin, et al. (2010). "Patient-specific induced pluripotent stem-cell models for long-QT syndrome." N Engl J Med **363**(15): 1397-1409.
- Nishishita, N., M. Shikamura, et al. (2012). "Generation of virus-free induced pluripotent stem cell clones on a synthetic matrix via a single cell subcloning in the naive state." PLoS One **7**(6): e38389.
- Odom, D. T., R. D. Dowell, et al. (2007). "Tissue-specific transcriptional regulation has diverged significantly between human and mouse." Nat Genet **39**(6): 730-732.
- Okabe, S., S. Fukuda, et al. (2002). "Activation of Wiskott-Aldrich syndrome protein and its association with other proteins by stromal cell-derived factor-1alpha is associated with cell migration in a T-lymphocyte line." Exp Hematol **30**(7): 761-766.
- Orange, J. S., N. Ramesh, et al. (2002). "Wiskott-Aldrich syndrome protein is required for NK cell cytotoxicity and colocalizes with actin to NK cell-activating immunologic synapses." Proc Natl Acad Sci U S A **99**(17): 11351-11356.
- Orange, J. S., K. D. Stone, et al. (2004). "The Wiskott-Aldrich syndrome." Cell Mol Life Sci **61**(18): 2361-2385.
- Patel, S. R., J. H. Hartwig, et al. (2005). "The biogenesis of platelets from megakaryocyte proplatelets." J Clin Invest **115**(12): 3348-3354.

- Prislovsky, A. and T. S. Strom (2013). "Increased uptake by splenic red pulp macrophages contributes to rapid platelet turnover in WASP(-) mice." Exp Hematol **41**(9): 789-798.
- Prislovsky, A., X. Zeng, et al. (2013). "Platelets from WAS patients show an increased susceptibility to ex vivo phagocytosis." Platelets **24**(4): 288-296.
- Pruksananonda, K., R. Rungsiwiwut, et al. (2012). "Eighteen-year cryopreservation does not negatively affect the pluripotency of human embryos: evidence from embryonic stem cell derivation." Biores Open Access **1**(4): 166-173.
- Risueno, R. M., E. Sachlos, et al. (2012). "Inability of human induced pluripotent stem cell-hematopoietic derivatives to downregulate microRNAs in vivo reveals a block in xenograft hematopoietic regeneration." Stem Cells **30**(2): 131-139.
- Robinton, D. A. and G. Q. Daley (2012). "The promise of induced pluripotent stem cells in research and therapy." Nature **481**(7381): 295-305.
- Sabri, S., A. Foudi, et al. (2006). "Deficiency in the Wiskott-Aldrich protein induces premature proplatelet formation and platelet production in the bone marrow compartment." Blood **108**(1): 134-140.
- Schwer, H. D., P. Lecine, et al. (2001). "A lineage-restricted and divergent beta-tubulin isoform is essential for the biogenesis, structure and function of blood platelets." Curr Biol **11**(8): 579-586.
- Snapper, S. B. and F. S. Rosen (1999). "The Wiskott-Aldrich syndrome protein (WASP): roles in signaling and cytoskeletal organization." Annu Rev Immunol **17**: 905-929.
- Soldner, F. and R. Jaenisch (2012). "Medicine. iPSC disease modeling." Science **338**(6111): 1155-1156.
- Suetsugu, S., H. Miki, et al. (1999). "Identification of two human WAVE/SCAR homologues as general actin regulatory molecules which associate with the Arp2/3 complex." Biochem Biophys Res Commun **260**(1): 296-302.
- Sullivan, K. E., C. A. Mullen, et al. (1994). "A multiinstitutional survey of the Wiskott-Aldrich syndrome." J Pediatr **125**(6 Pt 1): 876-885.

- Suzuki, N., S. Yamazaki, et al. (2013). "Generation of engraftable hematopoietic stem cells from induced pluripotent stem cells by way of teratoma formation." Mol Ther **21**(7): 1424-1431.
- Tablin, F., M. Castro, et al. (1990). "Blood platelet formation in vitro. The role of the cytoskeleton in megakaryocyte fragmentation." J Cell Sci **97 (Pt 1)**: 59-70.
- Takahashi, K., K. Tanabe, et al. (2007). "Induction of pluripotent stem cells from adult human fibroblasts by defined factors." Cell **131**(5): 861-872.
- Takahashi, K. and S. Yamanaka (2006). "Induction of pluripotent stem cells from mouse embryonic and adult fibroblast cultures by defined factors." Cell **126**(4): 663-676.
- Takayama, N., H. Nishikii, et al. (2008). "Generation of functional platelets from human embryonic stem cells in vitro via ES-sacs, VEGF-promoted structures that concentrate hematopoietic progenitors." Blood **111**(11): 5298-5306.
- Thon, J. N. and J. E. Italiano, Jr. (2012). "Does size matter in platelet production?" Blood **120**(8): 1552-1561.
- Thon, J. N., H. Macleod, et al. (2012). "Microtubule and cortical forces determine platelet size during vascular platelet production." Nat Commun **3**: 852.
- Thon, J. N., A. Montalvo, et al. (2010). "Cytoskeletal mechanics of proplatelet maturation and platelet release." J Cell Biol **191**(4): 861-874.
- Thrasher, A. J. and S. O. Burns (2010). "WASP: a key immunological multitasker." Nat Rev Immunol **10**(3): 182-192.
- Tiscornia, G., E. L. Vivas, et al. (2011). "Diseases in a dish: modeling human genetic disorders using induced pluripotent cells." Nat Med **17**(12): 1570-1576.
- Torres, E. and M. K. Rosen (2006). "Protein-tyrosine kinase and GTPase signals cooperate to phosphorylate and activate Wiskott-Aldrich syndrome protein (WASP)/neuronal WASP." J Biol Chem **281**(6): 3513-3520.
- Zhang, J., A. Shehabeldin, et al. (1999). "Antigen receptor-induced activation and cytoskeletal rearrangement are impaired in Wiskott-Aldrich syndrome protein-deficient lymphocytes." J Exp Med **190**(9): 1329-1342.

Zhu, Q., M. Zhang, et al. (1995). "The Wiskott-Aldrich syndrome and X-linked congenital thrombocytopenia are caused by mutations of the same gene." Blood **86**(10): 3797-3804.

Zou, J., C. L. Sweeney, et al. (2011). "Oxidase-deficient neutrophils from X-linked chronic granulomatous disease iPS cells: functional correction by zinc finger nuclease-mediated safe harbor targeting." Blood **117**(21): 5561-5572.





VITA

Name: Praewphan Ingrungruangleert

Address: 204 Moo7 Banglen Nakornpathom, THAILAND 73130

Telephone: 6683-1583073, 6634-301626

Email: numtip_in@hotmail.com

PERSONAL INFORMATION

Date of Birth: 8 August 1984

Place of Birth: Bangkok, Thailand

Marital Status: Single

EDUCATION

2010-present Ph.D. candidate, Program in Medical science, Faculty of Medicine, Chulalongkorn University, Thailand

2006-2009 M.Sc. (Medical science) Faculty of Medicine, Chulalongkorn University, Thailand

Thesis title: The effect of N-cadherin expressed in stromal cell derived osteoblast on hematopoietic stem cell properties.

2002-2005 B.Sc. (Biotechnology), (2nd class honor) Faculty of Engineering and Industrial technology, Silpakorn University, Nakornpathom, Thailand

Presentation

Oral presentation

1. Ingrungruangleert P., Israsena N. (Oct 15-17, 2009) "The effect of interferon alpha on DKK1 expression in marrow stromal cell" oral presentation at The 35th Congress on Science and Technology of Thailand (STT35), Burapra University, Chonburi, Thailand